Control of homeostasis of Dendritic Cells by the GTPase RhoA

Dissertation

zum Erwerb des Doktorgrades der Naturwissenschaften (Dr. rer. nat.)

an der Medizinischen Fakultät

der Ludwig-Maximilians-Universität München

vorgelegt von

Shuai Li

aus Linfen, Shanxi, China

2015

Gedruckt mit Genehmigung der Medizinischen Fakultät der

Ludwig-Maximilians-Universität München

Betreuer: Prof. Dr. Thomas Brocker

Zweitgutachter: Prof. Dr. Rainer Haas

Dekan: Prof. Dr. med. dent. Reinhard Hickel

Tag der mündlichen Prüfung: 17.03.2016

Author's declaration

Ich versichere hiermit ehrenwörtlich, daß die vorgelegte Dissertation "Control of homeostasis and Dendritic Cell survival by the GTPase RhoA" von mir selbständig und ohne unerlaubte Hilfe angefertigt wurde. Ich habe mich dabei keiner anderen als der von mir ausdrücklich bezeichneten Hilfen und Quellen bedient.

Die Dissertation wurde in der jetzigen oder ähnlichen Form bei keiner anderen Hochschule eingereicht und hat auch noch keinen anderen Prüfungszwecken gedient.

Shuai Li

TABLE OF CONTENTS

1. SUMMARY

Lymphoid and non-lymphoid tissues accommodate defined numbers of dendritic cells (DCs). There, DC-life span is influenced by various components such as proliferation and cell division triggered by cytokines, maturation processes in response to extracellular inflammatory and microbial substances, as well as induction of migration and apoptosis. Previous work has demonstrated the importance of specific numbers of DCs in tissues, as changes of DC numbers or DC life span could alter immunity, tolerance or inflammation resulting in various immune diseases. However, currently it is still unknown how DC life span and homeostasis is regulated *in vivo*.

RhoA is a member of Rho GTPase-family, which plays important roles in regulating cytoskeleton organization, proliferation, migration and survival. However, our current knowledge about RhoA-functions is based mostly on studies using dominant negative and constitutively active RhoA-mutants, which have possible unspecific effects on other members of the Rho GTPase family. Therefore, we used a LoxP/Cre recombinase approach to knock out RhoA selectively in DCs. Here we found that GTPase RhoA controlled the homeostasis of mature DCs, and deletion of RhoA caused significantly reduced numbers of $CD8^+CD11b^-$ and $CD11b^+Esam^{hi}$ DC subsets, while $CD11b^+Esam^{lo}$ DCs remained largely unaltered. Loss of RhoA interfered with homeostatic proliferation, cytokinesis, survival and turnover of cDCs. By performing proteomic analysis, we found that a pro-survival PI3Kγ/Akt/BAD pathway was deregulated in RhoA-ko DCs. Taken together, our findings indicate that RhoA plays a critical role in regulating DC-homeostasis, deletion of which decreases DC numbers resulting in impaired immune protection.

2. ZUSAMMENFASSUNG

Sowohl lymphoide, als auch nicht-lymphoide Organe beherbergen eine definierte Anzahl von dendritischen Zellen in speziellen Nischen. Dort wird die Lebensspanne der dendritischen Zellen von vielen Parametern, wie Proliferation und Zellteilung, die durch Zytokine gesteuert wird, Reifungsprozessen, die durch extrazelluläre entzündliche oder mikrobielle Substanzen reguliert werden, und durch Auswanderung oder Apoptose beeinflusst.

Frühere Arbeiten konnten zeigen, dass eine genau definierte Anzahl dendritischer Zellen in Geweben eine große Rolle spielt, da eine experimentell veränderte Zellzahl starke Auswirkungen auf Immunität, Toleranz oder Entzündungen hatten, was in verschiedenen Immunkrankheiten resultierte.

Allerdings sind die molekularen Mechanismen, welche die Homeostase und Lebensspanne von dendritischen Zellen regulieren, noch immer unklar.

RhoA, ein Mitglied der Rho-GTPase-Familie, ist wichtig für die Organisation der Zytoskeletts, Proliferation, Wanderung und Überleben von Zellen. Allerdings beruht unser momentanes Wissen über RhoA auf Studien, die dominant-negative und konstitutiv-aktive RhoA-Mutanten verwendeten. Dabei ist nicht auszuschließen, dass die Mutanten unspezifische Effekte auf andere Mitglieder der Rho-GTPasen-Familie haben. Um dieses Problem zu umgehen, verwendeten wir einen LoxP/Cre-Rekombinase-Ansatz, um RhoA selektiv in dendritischen Zellen zu inaktivieren.

Dabei haben wir beobachtet, dass RhoA die Homeostase von dendritischen Zellen reguliert, und dass die Deletion von RhoA eine starke Reduktion von CD11b$^-$CD8$^+$ und CD11b$^+$Esam^{hi}-Subpopulationen von dendritischen Zellen bewirkt, während CD11b$^+$Esam^{lo} dendritische Zellen dadurch nicht beeinflusst werden.

Der Verlust von RhoA beeinträchtigt die homeostatische Proliferation, Zytokinese, Überleben und Umsatz von klassischen dendritischen Zellen. Proteom-Analysen förderten einen defekten Signalweg, der das Überleben von Zellen reguliert zu Tage. Durch die Abwesenheit von RhoA, wurde der PI3Kγ/Akt/BAD Signalweg gestört.

Zusammenfassend lässt sich schlussfolgern, dass unsere Resultate RhoA als zentralen Regulator der dentrischen Zell-Homeostase identifizieren, dessen Deletion die Zahl der dendritischen Zellen unter die kritische Schwelle, die für einen effizienten Immunschutz notwendig ist, reduziert.

3. INTRODUCTION

3.1 Dendritic cells

Since Ralph Steinman and Zanvil Cohn first discovered dendritic cells (DCs) in the late 1970s (Steinman and Cohn, 1973, 1974), DCs have been known as most powerful antigen presenting cells that bridge innate and adaptive immunity. DCs are widely distributed throughout the body and specialized for uptake, processing and presentation of antigens to T cells (Shortman and Liu, 2002). Immature DCs (iDCs) act as sentinels in peripheral tissues that continuously sample environmental antigens and pathogens. Upon encounter of pathogen, DCs will take up those foreign antigens and migrate into draining lymph nodes (dLNs). Meanwhile, DCs undergo a maturation process and up-regulate co-stimulatory molecules such as CD40, CD80 and CD86. After maturation, mature DCs (mDCs) greatly lose their ability of taking up antigens but gain the powerful ability to process and present antigens to T cells. Therefore a protective immunity or tolerance is induced, depending on different DC subsets, maturation state and inflammatory signals (Reis e Sousa, 2006).

3.1.1 DC subsets

DCs are a heterogeneous group of cells that can be categorized into different subsets. The two main subsets are: plasmacytoid DCs (pDCs) and conventional or classic DCs (cDCs). pDCs are only a small population in the DC pool that share a similar origin with cDCs (Merad et al., 2013). However, compared to cDCs, pDCs are long-lived cells and widely distributed in lymphoid and non-lymphoid tissues (O'Keeffe et al., 2002). They are characterized by producing large amounts of type I interferons (IFNs) in response of viral infections (Liu, 2005; O'Keeffe et al., 2002; Yoneyama et al., 2004). pDCs express endosomal Toll-like receptor 7 and 9 (TLR7 and TLR9), which sense viral RNA and DNA respectively, therefore leading to type I IFN induction in order to clear viral infections (Guiducci et al., 2008). pDCs can be identified by their expression of Siglec-H and B220 on the cell surface (Zhang et al., 2006). The transcription factor E2-2 is specifically expressed in pDCs, which is critical for the development of pDCs, but not for cDCs (Cisse et al., 2008). It has been shown that E2-2 deficiency completely blocked the development of pDC by using E2-2 knockout (ko) mouse

model (Cisse et al., 2008). pDCs express only low levels of CD11c, MHC-II and costimulatory molecules in the steady state, which makes them inefficient in presenting antigens to T cells (Merad et al., 2013). However, their precise contribution to immunity is still unclear (Reizis et al., 2011).

cDCs are the typical DCs that Steinman originally discovered. They express high levels of CD11c, MHC-II and costimulatory molecules (CD40, CD80 and CD86), which are specialized for antigen processing and presentation. cDCs include several subsets that vary in phenotype and function (Diao et al., 2006). In lymphoid tissues, there are two major cDC subsets, CD8$^+$ DCs and CD11b$^+$ DCs. CD8$^+$ DCs represent around 20-40% of spleen and dLNs cDCs, but around 70% of thymus DCs (Henri et al., 2001; Vremec et al., 2000). The biggest difference between those two DC subsets is that CD8$^+$ DCs can effectively cross-present antigens via MHC-I molecules to CD8$^+$ T cells (Shortman and Heath, 2010), while CD11b$^+$ DCs are more efficient in activating CD4$^+$ T cells although both DC subsets can present antigens via MHC-II molecules (Dudziak et al., 2007; Lin et al., 2008). On the other hand, CD8$^+$ DCs produce high levels of IL-12 (Hochrein et al., 2001), which makes CD8$^+$ DCs, rather than CD11b$^+$ DCs, drive Th1 T cell responses (Maldonado-Lopez et al., 1999; Pulendran et al., 1999). The capacity of producing high amount of IL-12 and cross-presentation of exogenous antigens allows CD8$^+$ DCs to induce cytotoxic T cell (CTL) responses. Thus CD8$^+$ DCs are capable of engulfing dead cells, and cross-presenting cell-associated antigens on MHC-I molecules to CD8$^+$ T cells *in vivo* (Iyoda et al., 2002; Schulz and Reis e Sousa, 2002). In spleen, CD11b$^+$ DCs are comprised of two distinct Esam^{hi} and Esam^{lo} subsets, according to their expression of endothelial cell-specific adhesion molecule (ESAM) on cell surface (Lewis et al., 2011). CD11b$^+$Esam^{hi} DCs show typical DC morphology and surface maker expression profile, which are specialized for CD4$^+$ T cell priming (Lewis et al., 2011). CD11b$^+$Esam^{lo} DCs preferentially express monocyte-specific genes such as Ly6c, colony-stimulating factor 1 receptor (Csf1r), Csf3r and chemokine receptor CCR2, showing a pro-inflammatory cytokine response (Lewis et al., 2011). Notch2 is specifically required for the development of CD11b$^+$Esam^{hi} DCs, while Esam^{lo} counterparts are Notch2 independent (Lewis et al., 2011). Besides Notch2, some other pathways are also required for the development of CD11b$^+$Esam^{hi} DCs, including lymphotoxin-β receptor (LTβR), retinoic acid (RA) and chemotactic receptor EBI2 signaling (Gatto et al., 2013; Kabashima et al., 2005; Klebanoff et al., 2013; Yi and

Cyster, 2013). Furthermore, Notch2-dependent CD11b$^+$Esam^{hi} DCs derive from DC precursors, while CD11b$^+$Esam^{lo} DCs are thought to derive from circulating monocytes or earlier monocytic progenitors (Lewis et al., 2011). However, the precise origin of CD11b$^+$Esam^{lo} DCs is still unknown.

3.1.2 DC homeostasis

cDCs play a critical role in both the priming of T cell immune responses and the induction of self-tolerance. On one hand, cDCs capture and present foreign antigens to T cells, therefore initiating adaptive immunity. On the other hand, cDCs could also process and present self-antigen to induce tolerance. To maintain a balance between immunity and tolerance, it is crucial to keep normal numbers of cDCs with defined life spans in lymphoid organs. Previous studies have shown that constitutive ablation of cDCs or reduced cDC life spans led to defective priming of T cell response (Hou and Van Parijs, 2004; Jung et al., 2002; Ohnmacht et al., 2009; Park et al., 2006). Reduced CD4$^+$ DC-subset results in impaired CD4$^+$ T cell priming in EBI2 deficient mice (Yi and Cyster, 2013). Moreover, lack of cDCs also leads to inflammation and myeloproliferation (Birnberg et al., 2008), as well as T cell-mediated autoimmunity (Ohnmacht et al., 2009). Conversely, increased numbers of cDCs through inhibiting DC apoptosis, would lead to hyperactive B and T cell responses and autoimmunity due to defective tolerance induction (Chen et al., 2007; Chen et al., 2006; Nopora and Brocker, 2002; Stranges et al., 2007). These studies above indicate the importance of maintaining cDC homeostasis *in vivo*. However, it is still unclear which molecular mechanism controls the cDC homeostasis *in vivo*.

To maintain the homeostasis of a defined numbers of cDCs, the cDC pools in lymphoid organs need to get constant replenishment by DC precursors from the circulation (Liu et al., 2007). cDCs were initially thought to be non-dividing cells in lymphoid organs (Kamath et al., 2002; Kamath et al., 2000; Nopora and Brocker, 2002; Ruedl et al., 2000). However, recent studies have shown that about 5% of cDCs in spleen are proliferating at any time (Kabashima et al., 2005; Liu et al., 2007). Therefore, cDCs *in situ* proliferation also plays an important role in maintaining cDCs homeostasis in spleen. Since cDCs have a rapid turnover rate (half-life, 3 days) in spleen (Kamath et al., 2000), cell cycle control might also play a role in regulating

cDC generation from their circulating progenitor cells. Therefore, in order to fully understand mechanisms of DC homeostasis maintenance, it is important to find out how *in situ* proliferation and cell cycle is regulated in cDC.

3.1.2 DC ontogeny

Most DCs originate from hematopoietic stem cells in the bone marrow (BM). Hematopoietic stem cells can give rise to a progenitor called the macrophage and dendritic cell progenitor (MDP), which is the common precursor for monocytes, macrophages and DCs (Fogg et al., 2006) (Fig. 1). MDPs were initially identified as $Lin^-cKit^{lo}CX3CR1^+Flt3^+$ (Fogg et al., 2006). MDPs differentiate into monocytes and another progenitor called common DC progenitor (CDP) (Fig. 1), which is identified as $Lin^-cKit^{lo}CD115^+Flt3^+$ cell (Naik et al., 2007; Onai et al., 2007). CDPs exclusively give rise to cDCs and pDCs, but not monocytes or macrophages (Onai et al., 2007) (Fig. 1). In *in vitro* Flt3L-supplemented BM cultures, CDPs can be generated from BM cells, which were also called proDC (Naik et al., 2007). Then CDPs further give rise to a cDC-restricted precursor called pre-cDC, which can be recognized as $Lin^-CD11c^+MHC-II^-CD43^+Sirp\alpha^{int}$ in BM and spleen (Naik et al., 2006; Naik et al., 2007). These cells are able to differentiate into $CD8^+$ and $CD11b^+$ cDCs *in vivo* and *in vitro* (Naik et al., 2006; Naik et al., 2007). In steady state, pre-cDCs have been identified in BM (0.2%), blood (0.03%), lymph nodes (0.03%) and spleen (0.05%) with different frequencies (Liu and Nussenzweig, 2010; Liu et al., 2009). pDCs and pre-cDCs continually migrate through the blood into lymphoid tissues where these pre-cDCs further differentiate into $CD8^+$ and $CD11b^+$ cDCs (Liu et al., 2009) (Fig. 1). Pre-cDCs can also give rise to $CD103^+$ and $CD11b^+$ cDCs in skin, lung, kidney and intestine (Bogunovic et al., 2009; Ginhoux et al., 2009) (Fig. 1).

The granulocyte-macrophage colony-stimulating factor (GM-CSF) and fms-like tyrosine kinase 3 ligand (Flt3L) are two best-characterized cytokines regulating DC homeostasis. GM-CSF plays an important role in differentiation of hematopoietic progenitor cells (HPCs) into DCs *in vitro* (Caux et al., 1996; Inaba et al., 1992; Sallusto and Lanzavecchia, 1994). Injection of GM-CSF caused significantly increased numbers of DCs *in vivo,* suggesting its role in promoting DC expansion (Daro et al., 2000). Therefore, GM-CSF has widely been used for generating large numbers of DCs *in vitro*. However, lack of GM-CSF or GM-CSF receptor

(GM-CSFR) caused only a small decrease of DC numbers (Vremec et al., 1997). Interestingly, in GM-CSF or GM-CSFR deficient mice, CD103^{+} and CD11b^{+} DC subsets significantly decreased in non-lymphoid organs by apoptosis, indicating that GM-CSF can promote survival of those DC subsets (Greter et al., 2012; King et al., 2010; Kingston et al., 2009). Similar to GM-CSF, Flt3L is another critical cytokine required for the development of both pDCs and cDCs (Shortman and Naik, 2007). Injection of Flt3L dramatically increased DC numbers *in vivo* (Maraskovsky et al., 1996). Flt3 (also called CD135) is the receptor of Flt3L which is expressed on various DC-committed progenitor cells, such as MDPs, CDPs and pre-cDCs (Merad et al., 2013). In Flt3L- or Flt3-deficient mice, the numbers of DC progenitor cells, pDCs and cDCs were significantly decreased, while B and T cells remained unaltered (Kingston et al., 2009; McKenna et al., 2000; Waskow et al., 2008), suggesting its essential role in maintaining DC homeostasis. In addition, Flt3 also contributes to maintain normal numbers of DCs *in vivo* by regulating DC proliferation (Waskow et al., 2008).
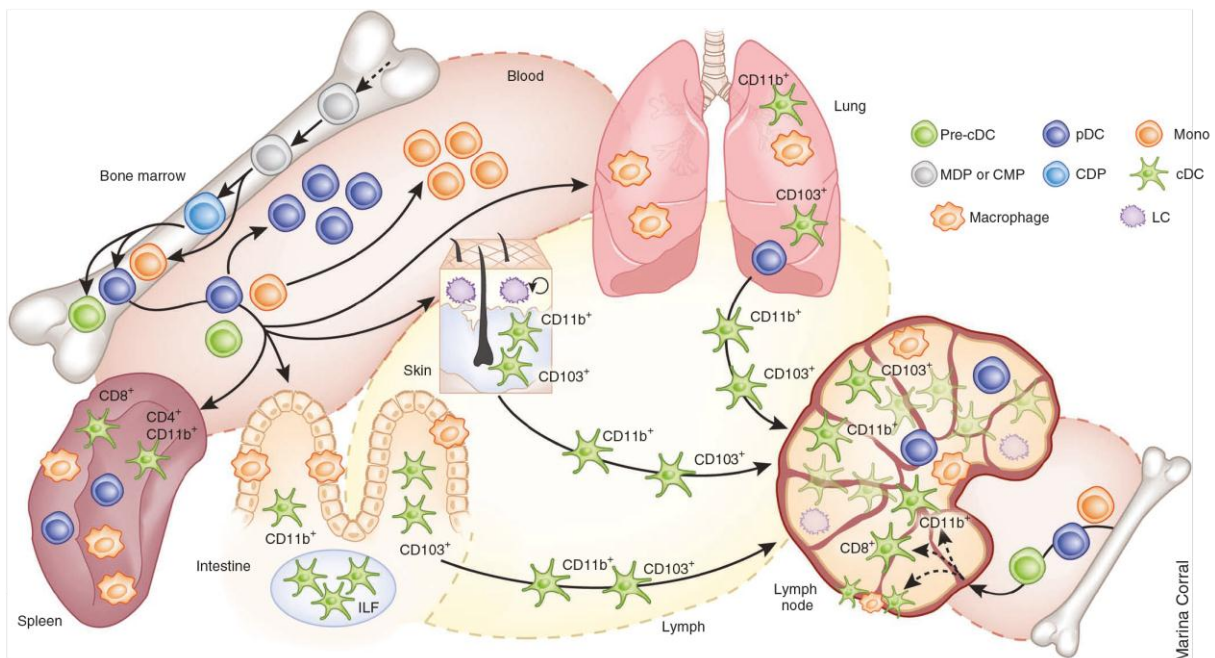
Figure 1. Development of DCs in steady state.
The cDCs, pDCs, and monocytes derive from MDPs in the BM. MDPs give rise to monocytes and CDPs, with the latter further develop into pDCs and pre-cDCs. Then monocytes, pDCs and pre-cDCs will migrate through blood and seed in lymphoid or non-lymphoid tissues, where pre-cDCs eventually differentiate into CD8^{+} (or CD103^{+}) and CD11b^{+} cDCs (Satpathy et al., 2012).

3.2 RhoA

Small Rho GTPases are a family of GTP-binding proteins that are found in all eukaryotic cells (Jaffe and Hall, 2005). The Rho GTPase family consists of 22 different members, in which RhoA, Cdc42 and Rac1 are the best characterized (Jaffe and Hall, 2005; Tybulewicz and Henderson, 2009). In this study, we mainly focus on RhoA functions in DCs. RhoA regulates multiple cellular functions in response to various external stimuli through cycling between inactive GDP-bound state and active GTP-bound state (Heasman and Ridley, 2008) (Fig. 2). Activation of RhoA is regulated by its specific guanine-nucleotide-exchange factors (GEFs), guanine nucleotide dissociation inhibitors (GDIs) and GTPase-activating proteins (GAPs) (Fig. 2). GEFs promote GTP binding to RhoA, which leads to RhoA activation. In contrast, both GAPs and GDIs cause RhoA inactivation through promoting hydrolysis of GTP and inhibiting GDP dissociation from RhoA respectively (Fig. 2). Activated RhoA recruits a variety of downstream effectors (e.g. ROCK, Citron kinase and mDia1) to regulate cytoskeleton organization, proliferation, migration and cell survival (Miller et al., 2012; Reuveny et al., 2004; Worthylake and Burridge, 2003) (Fig. 2).
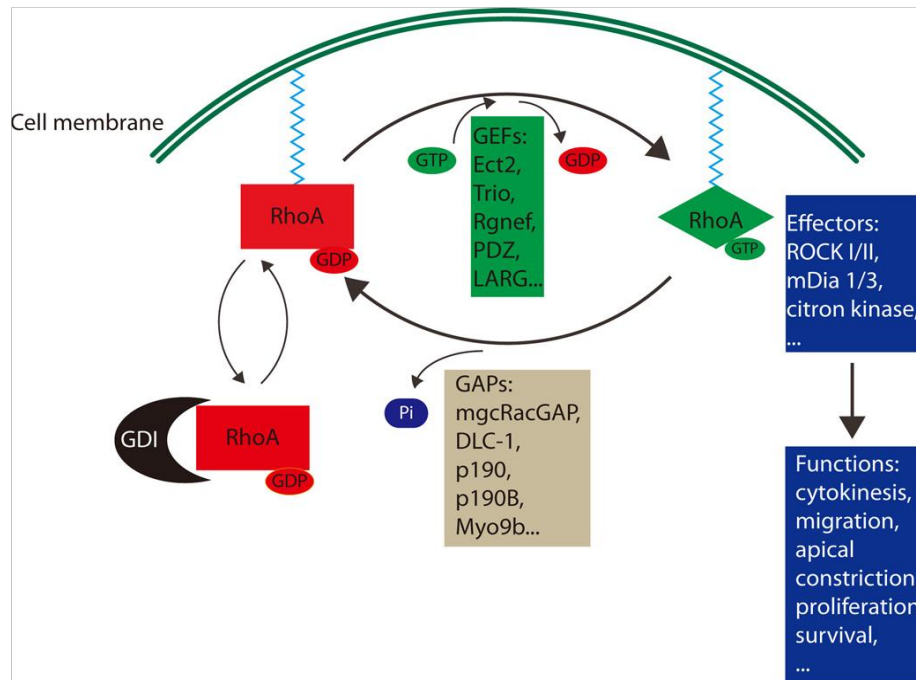
Figure 2. Activation and function of RhoA.
RhoA is cycling between the inactive GDP-bound state and active GTP-bound state in response of environmental stimuli. This cycling is tightly regulated by Rho guanine nucleotide exchange factors (GEFs), Rho GTPase-activating proteins (GAPs) and Rho GDP dissociation inhibitors (GDIs). Upon activation, the GTP-bound RhoA

can activate a large panel of downstream effectors to transduce signals that affect cell cytoskeleton organization, adhesion, cell cycle, survival and gene transcription (Zhou and Zheng, 2013).

Currently, most of our knowledge on RhoA functions is based on studies applying C3 transferase, overexpression of dominant-negative or constitutively active mutants to inhibit or excessively activate RhoA (Heasman and Ridley, 2008). However, these methods have nonspecific effects on other Rho GTPases. For example, C3 transferase inhibits activation of RhoA, as well as RhoB and RhoC, although it shows only a minor effect on other Rho GTPases (Cdc42 and Rac1) (Chardin et al., 1989; Mohr et al., 1992). And some studies have also revealed that overexpression of dominant negative mutants of RhoA may have nonspecific effects on Rac1 and/or Cdc42 (Heasman and Ridley, 2008; Wang and Zheng, 2007). Considering these limitations, it is necessary to apply RhoA specific ko models for RhoA functional studies. Recently, there have been several studies generating cell type specific RhoA-ko mice. In keratinocytes, RhoA deficiency did not affect skin development, but the contraction and directed migration of keratinocytes was markedly impaired (Jackson et al., 2011). In primary mouse embryonic fibroblasts (MEFs), deletion of RhoA led to significantly reduced proliferation due to defective cytokinesis (Melendez et al., 2011). RhoA deletion also caused strongly reduced B cells in lymphoid organs, suggesting its essential role in B cell development, however the proliferation of B cells was not affected (Zhang et al., 2012). Furthermore, RhoA deficiency resulted in a cytokinesis failure in HPCs, associated with accumulated multinucleated cells (Zhou et al., 2013). Obviously, these studies indicate that RhoA function is cell type dependent, and some of the previously proved cellular roles of RhoA might not be applied to other types of cells *in vivo*.

3.3 Aim of the project

In this study, we wanted to investigate functions of RhoA in DCs. Previous studies have shown that RhoA played an important role in the regulation of morphology and function of DCs by applying C3 toxin and a dominant-negative mutant (Kobayashi et al., 2001; Shurin et al., 2005). However, the specific role of RhoA in DCs is still largely unknown. So in our lab, we generated DC-specific RhoA-ko mice by crossing CD11c-Cre mice with RhoA floxed mice. With this mouse model, we were able to analyze if there were any defects in the development, migration, proliferation and survival of DCs in absence of RhoA and the underlying mechanisms behind those defects.

4. MATERIALS AND METHODS

4.1 Materials

4.1.1 Antibodies

4.1.1.1 Antibodies for flow cytometry

Specificity (anti-mouse)	Conjugate	Clone	Supplier
CD3e	PE	145-2C11	eBioscience
CD4	PE	GK1.5	BD Pharmingen
	PE-cy7	GK1.5	eBioscience
CD8a	PE	53-6.7	eBioscience
	Pacific-Blue		Invitrogen
	APC-eFluor 780	53-6.7	eBioscience
CD11b	APC-eFluor 780	M1/70	eBioscience
CD11c	FITC	N148	eBioscience
	PE	N148	eBioscience
	APC	N148	eBioscience
	PE-cy7	N148	eBioscience
CD16/32 (Fc block)		2.4G2	BD Pharmingen
CD19	PE	1D3	BD Pharmingen
CD40	APC	1C10	eBioscience
CD43	FITC	S7	BD Pharmingen
	Biotin	S7	BD Pharmingen
B220	PE	RA3-682	BD Pharmingen
CD45RA	PE	14.8	BD Pharmingen

CD45.1	FITC	A20	BD Pharmingen
	PE	A20	eBioscience
	Pacific Blue	A20	Biolegend
CD45.2	APC	104	Biolegend
CD80	PE	16-10A1	BD Pharmingen
CD86	PE	GL-1	eBioscience
CD103	PE	M290	BD Pharmingen
CD135 (Flt3)	PE	A2F10	eBioscience
	Biotin	A2F10	eBioscience
CD172α (Sirpα)	APC	P84	BD Pharmingen
NK1.1	PE	PK136	BD Pharmingen
Gr-1	PE	R86-8C5	BD Pharmingen
MHC-II (IA/IE)	FITC	M5/114.15.2	Biolegend
	PE	M5/114.15.2	eBioscience
	APC	M5/114.15.2	Biolegend
	Per-CP	M5/114.15.2	eBioscience
PDCA1	APC	129c1	Biolegend
Esam	PE	1G8	eBioscience
Ki67	PE	B56	BD Pharmingen
F4/80	PE	BM8	eBioscience
BrdU	FITC		BD Pharmingen
Ly6C	FITC	AL-21	BD Pharmingen
Streptavidin	Cy5	CALTAG	Life Technologies
	APC-cy7		BD Pharmingen

4.1.1.2 Antibodies for Western blot

Specificity	Host	Dilution	Supplier
β-actin	Rabbit	1/1000	Cell Signaling
RhoA	Rabbit	1/1000	Cell Signaling
PI3Kγ	Rabbit	1/1000	Cell Signaling
Akt	Rabbit	1/1000	Cell Signaling
Phospho-Akt	Rabbit	1/1000	Cell Signaling
Bad	Rabbit	1/1000	Cell Signaling
Phospho-Bad	Rabbit	1/1000	Cell Signaling
Rabbit	Donkey	1/2000	Jackson Lab

4.1.2 Chemicals

Chemicals were purchased from Roth (Karlsruhe, Germany), Merck (Darmstadt, Germany) or Sigma-Aldrich (St. Louis, MO, USA) unless stated differently. All buffers were prepared with double distilled water (dH_2O).

4.1.3 Consumables

Cell strainer (100μm)	BD, San Jose, CA, USA
Mesh filter (41μm)	Reichelt Chemietechnik, Heidelberg, Germany
Disposable syringes (1ml)	Braun, Melsungen, Germany
Injection needles 26G	Terumo Medical Corporation, Tokyo, Japan
Tubes of 1.5 ml and 2.0 ml	Eppendorf, Hamburg, Germany
FACS 5 ml tubes	SARSTEDT, Nümbrecht, Germany
15 ml and 50 ml falcon tubes	Greiner, Frickenhausen, Germany
PCR tubes (0.2 ml)	Nunc, Wiesbaden, Germany

Other materials and plastic wares were purchased from BD, Nunc (Wiesbaden, Germany) and Greiner (Frickenhausen, Germany).

4.1.4 Devices

Analytic scale (Adventurer, Ohaus Corp., Pine Brooks, NJ, USA), automatic pipettors (Integra Biosciences, Baar, Switzerland), bench centrifuge (Centrifuge 5415 D, Eppendorf, Hamburg, Germany), CASY cell counter (Roche, Basel, Switzerland), centrifuge (Rotixa RP, Hettich, Tuttlingen, Germany), chemical scale (Kern, Albstadt, Germany), flow cytometer (FACSCantoII, FACSAria, BD), incubator (Hera cell, Heraeus Kendro Laboratory Products, Hanau, Germany), laminar airflow cabinet (Heraeus), magnetic stirrer (Ika Labortechnik, Staufen, Germany), PCR-machine (Biometra, Goettingen, Germany), pH-meter (Inolab, Weilheim, Germany), pipettes (Greine, Frickenhausen, Germany), power supply (Amersham Pharmacia, Piscataway, NJ, USA), vacuum pump (KNF Neuberger, Munzingen, Germany), water bath (Grant Instruments Ltd., Barrington Cambridge, UK). All other devices are mentioned in the methods section.

4.1.5 Medium and solutions

ACK buffer	8.29 g NH_4Cl
	1 g $KHCO_3$
	37.2 mg Na_2EDTA
	H_2O ad 1 L
	pH 7.2-7.4 adjusted with 1 N HCl
	Sterilized by 0.2 μm filtration
BMDC medium	RPMI 1640 (PAA, Pasching, Austria)
	2 mM glutamine
	100 U/ml penicillin
	100 μg/ml streptomycin
	10% FCS
	20 ng/ml GM-CSF

PBS (Phosphate buffered saline)	150 mM NaCl
	10 mM Na_2HPO_4
	2 mM KH_2PO_4
	pH 7.4
	Adjusted with 5 N NaOH
FACS buffer	PBS
	2% FCS (v/v)
	0.01% NaN_3 (v/v)
MACS buffer	Dulbecco's PBS without Ca^{2+}/Mg^{2+} (Gibco)
	0.5% FCS (v/v)
	2 mM EDTA
50x TAE buffer	242 g Tris
	57.1 ml 100% acetic acid (v/v)
	100 ml 0.5 M EDTA
	pH 8.0
	H_2O ad 1 L
10x Gitocher buffer	670 mM Tris pH 8.8
	166 mM $(NH_4)_2SO_3$
	65 mM $MgCl_2$
	0.1 % Gelatin
Digestion mix for genotyping	1x Gitocher buffer
	0.5 % Triton-X
	1 % β-mercaptoethanol
	0.4 mg/ml Proteinase K
	H_2O

5x Cresol red buffer	250 mM KCl
	50 mM Tris/HCl pH 8.3
	43% glycerol
	2 mM Cresol-red
	7.5 mM $MgCl_2$

Western blot solutions:

Lysis buffer	50 mM Tris/HCl pH 8.8
	150 mM NaCl
	1 % NP40
	1/100 protease inhibitor cocktail
	1 mM PMSF
Running buffer	25 mM Tris Base
	192 mM Glycine
	0.1 % SDS
	H_2O
Separating gel 12%	30 % Acrylamid
	1.5 mM Tris/HCl pH 8.8
	1 % SDS
	1 % APS
	0.04 % TEMED
	H_2O
Stacking gel 5%	30 % Acrylamid
	1 M Tris/HCl pH 6.8
	1 % SDS

	1 % APS
	0.1 % TEMED
	H_2O
Transferring buffer	25 mM Tris-Base
	192 mM Glycine
	20 % Methanol
	0.002 % SDS
PBST	PBS
	0.05 % Tween-20
Blocking buffer	PBST
	5 % non-fat milk

4.1.6 Mice

All mice were bred and maintained at the animal facility of the Institute for Immunology (LMU, Munich) in accordance with established guidelines of the Regional Ethics Committee of Bavaria.

4.1.6.1 C57BL/6

C57BL/6 mice were originally obtained from the Jackson Laboratory (Bar Harbor, USA). C57BL/6 mice expressing congenic markers CD45.1 or CD45.2 were both used in this study.

4.1.6.2 RhoA-ko and CD11c-Cre mice

To generate mice with DC-specific RhoA deficiency, RhoA^{fl/fl} mice (Jackson et al., 2011) provided by Cord Brakebusch (University of Copenhagen, Copenhagen, Denmark) were crossed with CD11c-Cre mice (Caton et al., 2007) provided by Boris Reizis (Columbia University, New York, USA). These mice were abbreviated as RhoA-ko mice. CD11c-Cre mice were used as control mice in this study.

4.2 Methods

4.2.1 Cellular and immunological methods

4.2.1.1 Annexin V apoptosis detection

Apoptosis is a programmed cell death characterized by losing integrity of cell membrane. Annexin-V combined with 7-AAD is widely used to detect apoptotic cells due to its ability of binding to phosphatidylserine (PS). In viable cells, PS is located on the cytosolic side of cell membrane. When apoptosis occurs, PS flips to the extracellular of cell membrane, which can be detected by fluorescently labeled Annexin-V. In early stages of apoptosis, the cell membrane excludes viability dye 7-AAD, therefore Annexin-V single positive cells (7-AAD negative) are in early stages of apoptosis. During late-stage of apoptosis, 7-AAD can pass through cell membrane and bind the nuclei due to damaged cell membrane integrity. Therefore Annexin-V and 7-AAD double positive cells are in late stages of apoptosis.

4.2.1.2 BrdU pulse-chase

BrdU is an analog of thymidine that can be incorporated into newly synthesized DNA by proliferating cells. A specific anti-BrdU fluorescent antibody is used to detect cells incorporated BrdU. The percentages of BrdU-labeled cells are then measured by flow cytometry. To measure the DC turnover rate, a BrdU pulse-chase experiment is performed. During the pulse phase, BrdU is administrated, and the percentage of BrdU$^+$ DCs increases over time. During the BrdU-free chase phase, the percentage of BrdU$^+$ DCs declines over time. This provides information of DC turnover rate and DC longevity. Briefly, mice were injected intraperitoneally (i.p.) with 1 mg BrdU in 100 μl PBS, and then continuously received drinking water containing 0.8 mg/ml BrdU for 3 days. Then giving mice normal drinking water, at various time points, spleen cells were harvested and stained with antibodies against cell surface molecules. After washing, cells were fixed and permeabilized with cytofix/cytoperm buffer (BD Bioscience). Following washing, cells were incubated with DNase I for 1h at 37 °C. The cells were then incubated at RT with FITC conjugated BrdU antibody (BD Biosciences, San Diego, CA) for 30 minutes. After washing, cells were re-

suspended and analyzed by flow cytometry.

4.2.1.3 Flow cytometry and cell sorting

Flow cytometry (Fluorescence-Activated Cell Sorting, FACS) is a method that can evaluate various cell characteristics such as cell size (forward scatter, FSC), granularity (side scatter, SSC) and marker expression. Single cell suspensions are stained with fluorescent antibodies against cell surface or intracellular antigens. Antibodies labeled cells pass by a laser beam and then several detectors. A variety of cell information such as FCS, SSC and fluorescence intensity are acquired and used to analyze immune cell phenotype and functions.

In brief, $2x10^6$ cells were placed into a V-bottom 96 well plate and washed with PBS. Cells were incubated with 50 μl of FACS buffer containing certain fluorescent antibodies for 20 min at 4 ℃ in the dark. To remove unbound antibodies, cells were washed with FACS buffer, and then re-suspended in 150 μl FACS buffer. Cells stained with biotinylated antibodies can be further detected with a fluorescent streptavidin in a second staining step. For intracellular staining, cells are fixed and permeabilized first with BD Cytofix/Cytoperm buffer according to the manufacturer's protocol. Data were acquired through running samples in FACSCanto II (BD Bioscience) with three lasers (488, 633 and 405 nm).

Cell sorting is an advanced flow cytometry used to identify and collect certain interest cell populations. By using FACSAria instrument (BD), the population of interest can be identified and electrical charged, and then collected by electrostatic droplet deflection. FACS data were analyzed with FlowJo software (TreeStar, Ashland, OR, USA).

4.2.1.4 Histology

Spleens were embedded in O.C.T. compound (Sakura Finetek) and frozen immediately in liquid nitrogen. Spleens were cut into 5 μm sections using a cryostat at -15 ℃ (Jung Frigocut 2800 E, Leica) and air-dried overnight at RT. Spleen sections were fixed with ice-cold acetone at -20 ℃ for 10 min, then air-dried for at least 1 hour. After 15 min rehydrate in PBS containing 0.25% BSA, sections were blocked in PBS containing 0.25% BSA and 10% mouse serum for 15 min at RT. After blocking, spleen sections were incubated with rat anti-mouse

CD8-FITC, CD11c-PE, B220-APC and Moma-Biotin antibodies for 30 min at RT. After washing, sections were further stained with streptavidin-cy5 for 30 min at RT. Then spleen sections were directly mounted in Fluoromount-G (SouthernBiotech) after washing. At last, spleen sections were visualized using an Olympus BX41TF-5 microscope equipped with F-View II Digital Micro camera (Olympus).

4.2.1.5 ImageStream

The ImageStream is a novel technology that combines advantages of flow cytometry and microscopy. It can provide both accurate statistical analysis and images of cells at the same time. ImageStreamX Mark-II (Amnis Corporation, Seattle, WA, USA) equipped with 5 lasers (405, 488, 561, 642 and 785 nm) is capable of detecting side scatter, bright field, and 4 fluorescent channels.

For cell cycle analysis, $3x10^6$ BMDCs or *ex vivo* isolated spleen DCs were stained with antibodies against surface markers at 4 ℃ for 20 min. After washing, cells were fixed in Cytofix/Cytoperm buffer at 4 ℃ for 30 min. Then, the nuclei were stained with DAPI in Perm/Wash buffer at 4 ℃ for 10 min. After washing, cells were re-suspended with 50 μl PBS and analyzed by ImageStreamX Mark-II. 100,000 cells of each sample were recorded. Flow cytometry and image data were acquired and analyzed by Amnis INSPIRE and IDEAS software respectively. Different populations can be discriminated based on combined features of size, shape, fluorescent intensity, etc.

4.2.1.6 Generation of BMDC and Flt3L-DC

Bone marrow derived DCs (BMDCs) are generated from BM cells in the presence of GM-CSF. Femur and tibiae were taken from mice, and BM cells were flushed out using a 0.45x12 mm needle with BMDC-medium (see 4.1.5). Red blood cells were lysed in ACK buffer (see 4.1.5) for 2 min at RT. Then $10\text{-}15x10^6$ cells were cultured in 20 ml BMDC-medium per 100mm plate for 10-13 days. The medium was refreshed at day3 and 7. The purity and maturation level of BMDCs were analyzed by flow cytometry based on the expression of CD11c, MHC-II, CD40 and CD86.

Flt3L-derived DCs were generated from BM cells as well in the presence of Flt3L. BM was extracted from femur and tibiae, and red blood cells were lysed in ACK buffer. BM cells were cultured at $1x10^6$ cells/ml in RPMI 1640 medium (with 10% FCS, Pen-Streptomycin and 50μM 2-mercaptoethanol) in the presence of 20 ng/ml homemade recombinant murine Flt3L. At day 3, cells were collected and used for pro-DC and pre-cDC sorting as described (Naik et al., 2007).

4.2.1.7 Magnetic cell sorting (MACS)

MACS is a technique used for isolating different cell subpopulations according to their specific surface markers. First, the target cells are labeled with specific monoclonal antibodies that are conjugated to magnetic microbeads. Then, the cell suspension is loaded onto a MACS column, which is placed in the magnetic field of a MACS separator. The magnetically labeled positive cells are retained within the column. The unlabeled negative cells will run through the column. After removing from the magnetic field, the magnetically labeled positive cells can be eluted from column. Therefore, the positive and negative cells are collected separately.

In this study, MACS was utilized to isolate CD11c-positive DCs (CD11c microbeads, Miltenyi Biotec, Germany) from spleen. For DC precursor sorting, spleen cells were labeled with biotin-conjugated antibodies against lineage markers (CD3, CD19, B220 and NK1.1). Then streptavidin microbeads (Miltenyi Biotec, Germany) were used to isolate lineage negative cells by negative selection. The enriched lineage negative cells can be further used for pre-cDC sorting. All procedures were performed according to the manufacturer's instructions.

4.2.1.8 Mixed bone marrow chimera

BM cells were harvested from femurs and tibiae of CD11c-Cre (CD45.1) and RhoA-ko (CD45.2) donor mice 6-8 weeks of age. The red blood cells were lysed with ACK buffer, then $5x10^6$ total 50:50 mixed BM cells were injected intravenously (i.v.) into lethally irradiated (split dose: 600 rad at day -1 and 0) recipient B6 mice (CD45.2, 10-12 weeks of age). After BM transfer, recipient mice received drinking water containing 1.2 g/l of Neomycin for 4 weeks. Mixed BM chimeras were analyzed or used for BrdU pulse-chase experiment 8 weeks

after fully BM reconstitution.

4.2.1.9 Single cell suspension preparation

Lymph nodes (pooled axillary, brachial and inguinal, LNs), spleen and thymus were collected respectively, and enzymatically digested using a solution containing Liberase DL (0.125 mg/ml) and DNase I (0.2 mg/ml, both from Roche, Basel, Switzerland). After a 30 min digestion at 37°C, these organs were smashed and filtered through a cell strainer (100μm) to obtain a single cell suspension. The red blood cells were lysed using ACK buffer. Cell numbers were determined using CASY cell counter (Roche, Basel, Switzerland).

4.2.1.10 TUNEL assay

TUNEL (TdT-mediated dUTP-biotin nick end labeling) assay is usually used to detect DNA fragmentation in apoptotic cells. Fragmented DNA can be labeled with digoxigenin-nucleotide by using terminal deoxynucleotidyl transferase (TdT), and then detected with an anti-digoxigenin fluorescent antibody. TUNEL-positive DCs in spleen were detected using ApopTag Fluorescein In Situ Apoptosis Detection Kit (Millipore; Billerica, Massachusetts, USA) according to the manufacturer's instructions. Briefly, spleen cell suspension was first labeled with fluorescent antibodies against surface markers, and then cells were fixed in 1% paraformaldehyde in PBS for 30 minutes at RT. Cells were permeabilized with 0.1% Triton X-100 on ice for 2 minutes. After washing, cells were incubated with working strength TdT enzyme for 30 minutes at 37℃. The reaction was stopped using stop/wash buffer. After three washes in PBS, cells were incubated with anti-digoxigenin Fluorescein conjugate for 30 min at RT. And then the DNA of cells was stained with DAPI. TUNEL-positive DCs were detected by flow cytometry.

4.2.1.11 ELISA test of Flt3L

Serum levels of Flt3L in Cre control and RhoA-ko mice was measured using mouse Flt-3 Ligand ELISA kit (catalog #DY427, R&D system) according to the manufacturer's instructions. Serum was first diluted at 1:20, and then used for ELISA measurement. The optical density was determined at 450 nm with Kinetic ELISA Microplate Reader (Molecular

Devices, CA, USA).

4.2.2 Molecular biology methods

4.2.2.1 Agarose gel electrophoresis

Agarose gel electrophoresis is used to separate a mixed DNA fragments according to their size. A 100 bp DNA ladder (New England Biolabs, Ipswich, MA, USA) was applied to determine the size of different DNA fragments. DNA mixture was loaded onto a 1% of agarose gel and separated by applying a constant voltage to an electrophoresis chamber filled with TAE buffer (see 4.1.5). DNA was visualized under UV light by addition of ethidium bromide (0.5 μg/ml).

4.2.2.2 Polymerase chain reaction (PCR) and genotyping

PCR is a common molecular biology technology used to rapidly amplify a specific DNA sequence. In this study, PCR was used to check phenotypes of different mouse strains. Genomic DNA of mice was extracted by incubating a small piece of mouse tail in digestion buffer (see 4.1.5) at 55 ℃ for 6 hour, followed by deactivation of proteinase K at 95 ℃ for 5 min. The following primers were used to test Cre and RhoA flox gene:

Table 1: primers for genotyping

Cre	Forward	GGACATGTTCAGGGATCGCCAGGCG
	Reverse	GCATAACCAGTGAAACAGCATTGCTG
RhoA flox	Forward	AGCCAGCCTCTTGACCGATTTA
	Reverse	TGTGGGATACCGTTTGAGCAT

PCR mix:

0.2 μl forward primer (100 pmol/μl)

0.2 μl reverse primer (100 pmol/μl)

6 μl Cresol red buffer with $MgCl_2$ (see 4.1.5)

1.0 μl DNA

5 U/ml PANScript DNA polymerase

dH$_2$O ad 29 µl

PCR reactions were performed using the following program:

Step 1:	95 ℃	5 min	
Step 2:	95 ℃	30 sec	
Step 3:	55 ℃	30 sec	
Step 4:	72 ℃	30 sec	(back to step 2 for 35 cycles)
Step 5:	72 ℃	10 min	
Step 6:	4 ℃	Pause	

4.2.2.3 Isolation of mRNA and cDNA synthesis

Total RNA was extracted from 1x10^6 cells using the RNeasy Mini Kit (Qiagen, Hilden, Germany) according to manufacturer's instructions. The remaining DNA was removed by on-column DNase I digestion. The concentration and quality of RNA were measured by a NanoDrop spectrophotometer (NanoDrop Technologies, Wilmington, DE, USA). The mRNA was reverse transcribed into cDNA using the QuantiTect Reverse Transcription Kit (Qiagen) according to the instructions of manufacturer.

4.2.2.4 Quantitative PCR (qPCR)

qPCR is used to determine relative transcription of certain genes. In this study, the TaqMan probes were used for qPCR examination. The fluorescent-labeled TaqMan probes give a signal only after their binding to a specific cDNA sequence. The strength of signal is correlated with initial amount of cDNA. The cycle threshold (Ct) value represents minimal numbers of PCR cycle required for detectable signal strength.

The TaqMan assay was performed with the LightCycler TaqMan Master Kit and the Universal ProbeLibrary Set mouse (Roche) according to the manufacturer's instructions on a CFX96 Real Time System (Bio-Rad, Hercules, CA, USA). The primers and probes are listed in table 2. The housekeeping gene HPRT was used as endo-gene for normalizing. The relative expression of target genes was calculated by using the 2$^{-\Delta\Delta Ct}$ method.

Table 2. Primers and probes for qPCR

Genes	Primers	Sequence	Probe
HPRT	Forward	TCCTCCTCAGACCGCTTTT	95
	Reverse	CCTGGTTCATCATCGCTAATC	
RhoA	Forward	CCTGTGTGTTTTCAGCACCTT	46
	Reverse	ACCTCTGGGAACTGGTCCTT	
PI3Kγ	Forward	GGAGACTGAATCTCTGGACCTG	29
	Reverse	GTGGCATCCTTTACAATCTCG	
Ripk1	Forward	TACCTCCGAGCAGGTCAAAT	50
	Reverse	AAACCAGGACTCCTCCACAG	
Ripk3	Forward	CCGACGATGTCTTCTGTCAA	6
	Reverse	GACTCCGAACCCTCCTTTG	
Glud1	Forward	GGTCATCGAAGGCTACCG	76
	Reverse	TCAGTGCTGTAACGGATACCTC	
TNF-α	Forward	CCCCAAAGGGATGAGGTAGT	104
	Reverse	CTAACCCGTCTTGCTTGTGAG	
Fth1	Forward	GCCAGAACTACCACCAGGAC	75
	Reverse	CCACATCATCTCGGTCAAAAT	
TNFR1	Forward	TGTCAATTGCTGCCCTGTC	40
	Reverse	GATGTATCCCCATCAGCAGAG	

4.2.2.5 Western blot

Total proteins were extracted from 1×10^6 BMDCs or *ex vivo* isolated spleen DCs using protein lysis buffer (see 4.1.5). Concentrations of proteins were measured by Quant-iT protein assay kit (Invitrogen, Carlsbad, CA, USA). Proteins were denatured in a 5% SDS solution for 10 min at 95 ℃. 20-30 μg proteins were loaded and separated by SDS-PAGE (12%). After the

transfer to a nitrocellulose membrane, proteins were blocked in PBST (see 4.1.5) with 5% non-fat milk overnight at 4 ℃. The membrane containing proteins were washed in PBST and incubated with primary antibodies at RT for 1.5 hour. After washing, proteins were incubated with secondary HRP-labeled antibody at RT for 1h. The membrane was washed with PBST, then incubated with luminescent substrate ECL (Amersham, Piscataway, NJ) and visualized by the OPTIMAX film-developing machine (PROTEC Medizintechnik, Oberstenfeld, Germany). Western blot bands were quantified by imageJ software.

4.2.2.6 Proteomics

Proteomics was performed in collaboration with Stefan Lichtenthaler's group at the German Center for Neurodegenerative Diseases (DZNE) in Munich. Samples are prepared as described before (Wisniewski et al., 2009b). Briefly, $20x10^6$ BMDCs were lysed and sonified in a sonication bath. The lysates were then centrifuged at 13,000 rpm for 5 min. The supernatant containing proteins were collected and digested using the FASP method as described before (Wisniewski et al., 2009b). Protein peptides were fractionated into three fractions using strong anion exchange in a pipet-tip based format as described before (Wisniewski et al., 2009a). Protein fractions were desalted using home made C18 STAGE tips (Rappsilber et al., 2007). 3 μg of the fractionated peptides were injected per run. Samples were analyzed on an easy nLC liquid chromatography system and on the LTQ Velos Orbitrap Pro mass spectrometer using a homemade 15 cm column and 2 h gradients. 5 biological replicates with 2 technical replicates were analyzed using Cre control and RhoA-ko samples. The obtained raw data were subjected to label free quantitation using the freely available MaxQuant software. Statistical analysis was carried out in Perseus software. Only proteins with 2 or more unique peptides in at least 3 out of 5 biological were considered as identified proteins.

4.3 Statistical analysis

Statistical differences between the experimental groups were determined by Student's two-tailed t-test. Probabilities < 0.05 were considered to be significant.

5. RESULTS

5.1 Verification of RhoA knock out efficiency in DCs

In order to explore RhoA functions in DCs, we generated DC-specific RhoA-ko mice by crossing mice carrying loxP-flanked RhoA alleles (RhoAfl/fl) with CD11c-Cre mice (Fig. 3A). The Cre recombinase is selectively expressed in CD11c-positive DCs under the control of CD11c promoter (Fig. 3A). Cre will bind to LoxP sites and cut off exon 3 of RhoA gene specifically in DCs, leading to RhoA deletion (Fig. 3A). To verify the RhoA ko efficiency, a qPCR was performed to detect RhoA mRNA levels in BMDCs and *ex vivo* isolated spleen DCs. We found that RhoA mRNA was significantly decreased in both BMDCs and spleen DCs, however we were still able to detect low levels of residual RhoA mRNA (Fig. 3B). To further confirm RhoA knock out efficiency on protein level, we performed a Western blot by using total protein extracted from BMDCs and spleen DCs isolated via MACS. As shown in Figure 3C, RhoA protein has been effectively deleted from both RhoA-ko BMDCs and spleen DCs. Since the purity of CD11c$^+$ BMDCs is around 90%, the observed RhoA mRNA and protein residual may derive from non-DC cells, such as CD11c^{low} monocytes and macrophages.
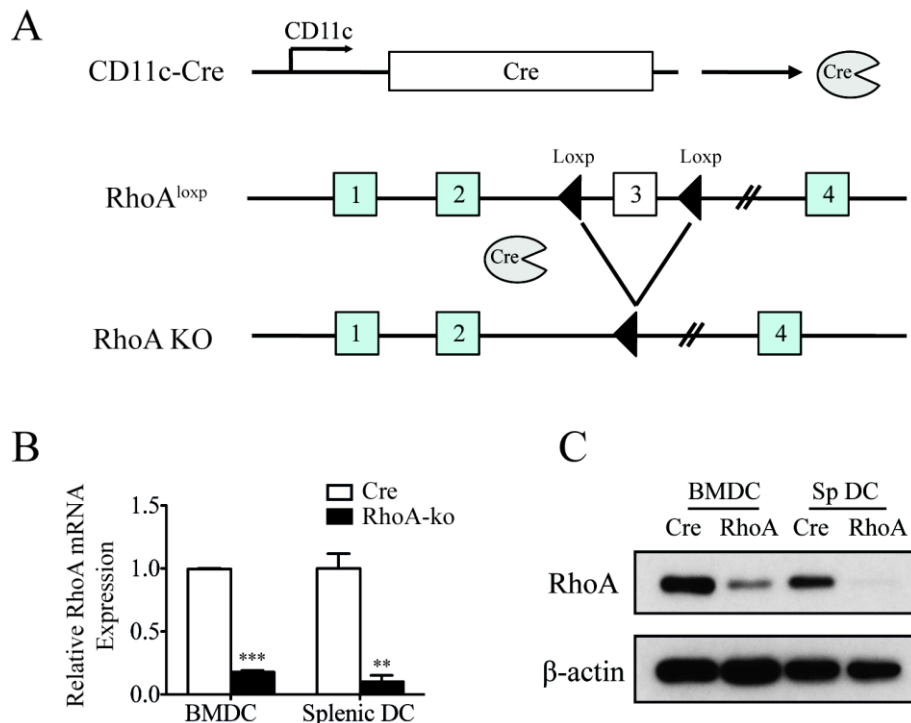
Figure 3. Generation and verification of RhoA ko in DCs.
(A) Cre is expressed specifically in DCs under the control of CD11c promoter. The exon 3 of RhoA allele is flanked with LoxP sequence. Upon Cre–mediated recombination, the RhoA exon 3 between two LoxP sites is excised, resulting in RhoA inactivation. (B) RhoA mRNA levels were determined by qPCR in BMDCs and spleen DCs. Relative RhoA mRNA levels were obtained by normalization to HPRT mRNA levels. Bars represent mean ±SEM (n=3). (C) RhoA protein expression in RhoA-ko BMDCs and spleen DCs were detected by Western blot. β-actin served as a protein loading control. Figures show representative data of one out of at least three experiments with similar outcome.

5.2 RhoA deletion results in reduced numbers of cDCs in spleen

To provide insights into the role of RhoA in DCs, we first characterized DC populations in RhoA-ko mice. In spleen, cDCs were identified as $CD11c^+MHC\text{-}II^+$ cells, which significantly decreased in RhoA-ko mice (Fig. 4A). The percentages of cDC significantly reduced in RhoA-ko mice compared to Cre controls (Fig. 4A). Further analyses of DC subsets showed that $CD11b^+$ cDCs had a more severe reduction in total cell numbers compared to $CD8^+$ cDCs (Fig. 4B). Recently, splenic $CD11b^+$ DCs have been shown to consist of two distinct $Esam^{hi}$ and $Esam^{lo}$ populations (Lewis et al., 2011). $CD11b^+Esam^{hi}$ DCs are pre-cDC-derived, and dependent on Notch2 and LTβR signaling with a higher turnover rate (Lewis et al., 2011; Wang et al., 2005; Yi and Cyster, 2013). $CD11b^+Esam^{lo}$ DCs are Notch2 independent and have a monocyte-derived origin (Lewis et al., 2011; Wang et al., 2005; Yi and Cyster, 2013). So we also analyzed $Esam^{hi}$ and $Esam^{lo}$ DC subsets within $CD11b^+$ DC compartment. $Esam^{hi}$ DCs dramatically decreased in spleens of RhoA-ko mice both in percentage and total cell numbers (Fig. 4A,B). However, the total number of $Esam^{lo}$ DCs remained unaltered in RhoA-ko mice (Fig. 4A,B). In addition, we also found the expression of CD4 strongly reduced in $CD11b^+$ DCs showing a similar effect as Esam marker by RhoA deletion (Fig. 4A). Our results indicate that RhoA deletion causes significant decrease in number of $CD8^+$ and $CD11b^+Esam^{hi}$ cDCs but not in $CD11b^+Esam^{lo}$ cDCs.

Previous studies have shown that $CD8^+$ cDCs were located mostly in T cell zones (Dudziak et al., 2007), while $CD11b^+$ cDCs were preferentially located in the red pulp of spleen (Yi and Cyster, 2013). Therefore, we wondered whether the positioning of those two DC subsets was altered by RhoA deletion. To test that, we performed histological analyses and found that the main structure of spleens in RhoA-ko mice remained intact, with normal T and B cell zones (Fig. 4C). Both $CD8^+$ and $CD11b^+$ cDCs were present in their proper location in spleens of RhoA-ko mice (Fig. 4C). However, the total numbers of both DC subsets were markedly

reduced in RhoA-ko mice (Fig. 4C), consistent with the finding from flow cytometry (Fig. 4A,B). This result indicates that deletion of RhoA did not affect the positioning of cDC, but caused significantly decreased numbers of cDC in spleen.
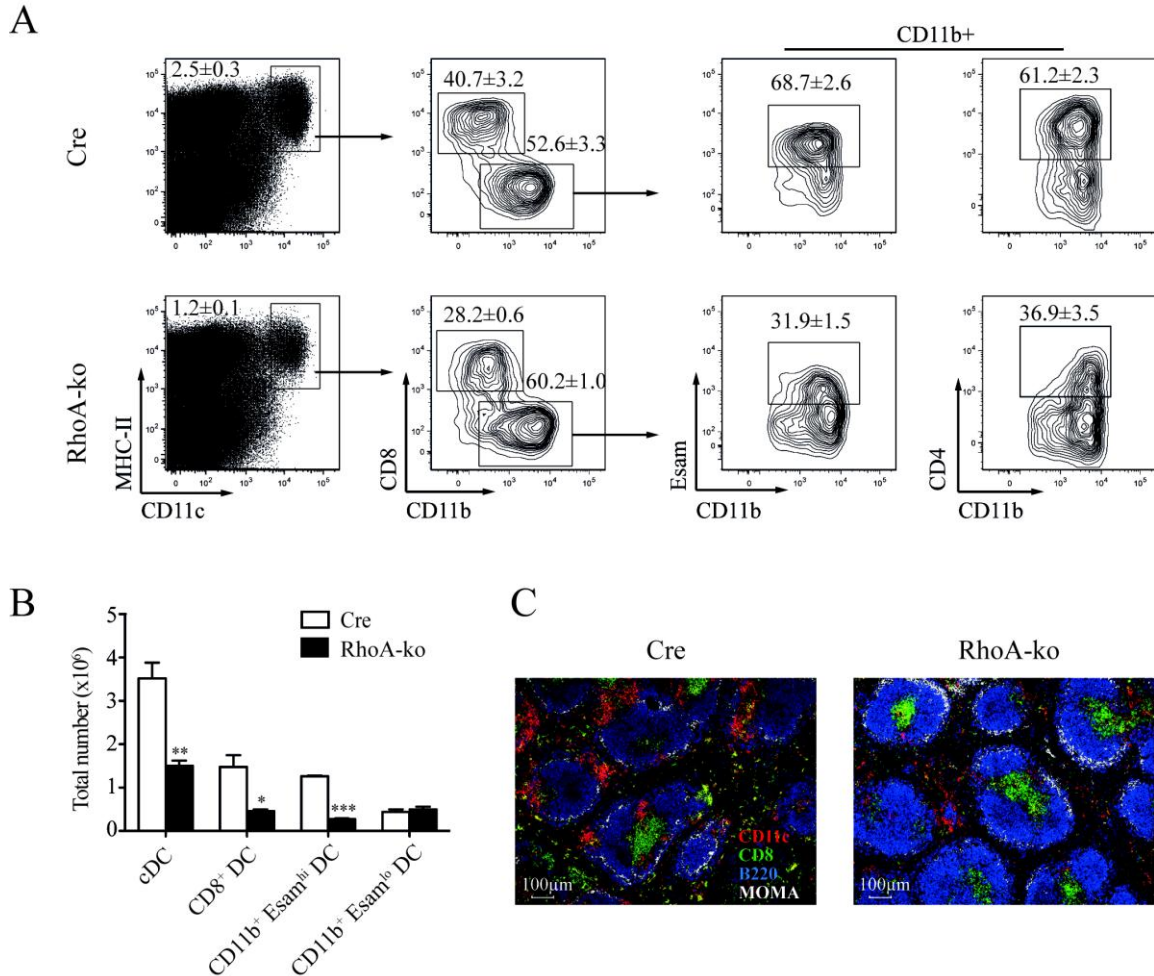
Figure 4. RhoA is essential for the homeostasis of DCs in spleen.
(A) cDCs are identified as CD11c$^+$MHC-II$^+$ in spleen. cDCs can be separated into CD8$^+$ and CD11b$^+$ DC subsets. Expression of Esam and CD4 was further analyzed in CD11b$^+$ DC compartment. The percentages represent mean $\pm$ SEM (n=3). (B) Bar graphs show total cell numbers of cDC and different DC subsets (n=3). (C) Histology staining identified B cells (B220$^+$, blue), CD8$^+$ T cells (CD8$^+$, green), marginal zone macrophages (MOMA$^+$, white) and cDCs (CD11c$^+$, red) in the spleen of Cre control and RhoA-ko mice. Figures show representative data of one out of at least six experiments with similar outcome.

5.3 RhoA deletion results in number reduction of cDCs in lymph nodes and thymus

In lymph nodes, both migratory (MHC-II high) and resident (MHC-II intermediate) cDCs were markedly decreased in RhoA-ko mice (Fig. 5A). Resident DCs can be divided into CD8$^+$

and CD11b$^+$ DC subsets. The total number of resident CD8$^+$ DC was significantly reduced, while CD11b$^+$ DCs remained largely unaltered in RhoA-ko mice (Fig. 5A). Migratory DCs can be divided into three subsets CD103$^+$CD11b$^-$, CD103$^-$CD11b$^+$ and CD103$^-$CD11b$^-$ DCs. In RhoA-ko mice, all of these migratory DC subsets were significantly reduced in total number (Fig. 5A). In thymus, cDCs are identified as CD45RA$^-$CD11c$^+$, while pDCs are identified as CD45RA$^+$CD11c^{int} (Onai et al., 2013)(Fig. 5B). As shown in Figure 5B, the total number of cDC was significantly decreased in thymus of RhoA-ko mice, while pDC remained unaffected by RhoA deficiency. Our results indicate that cDCs significantly decreased also in lymph nodes and thymus of RhoA-ko mice.
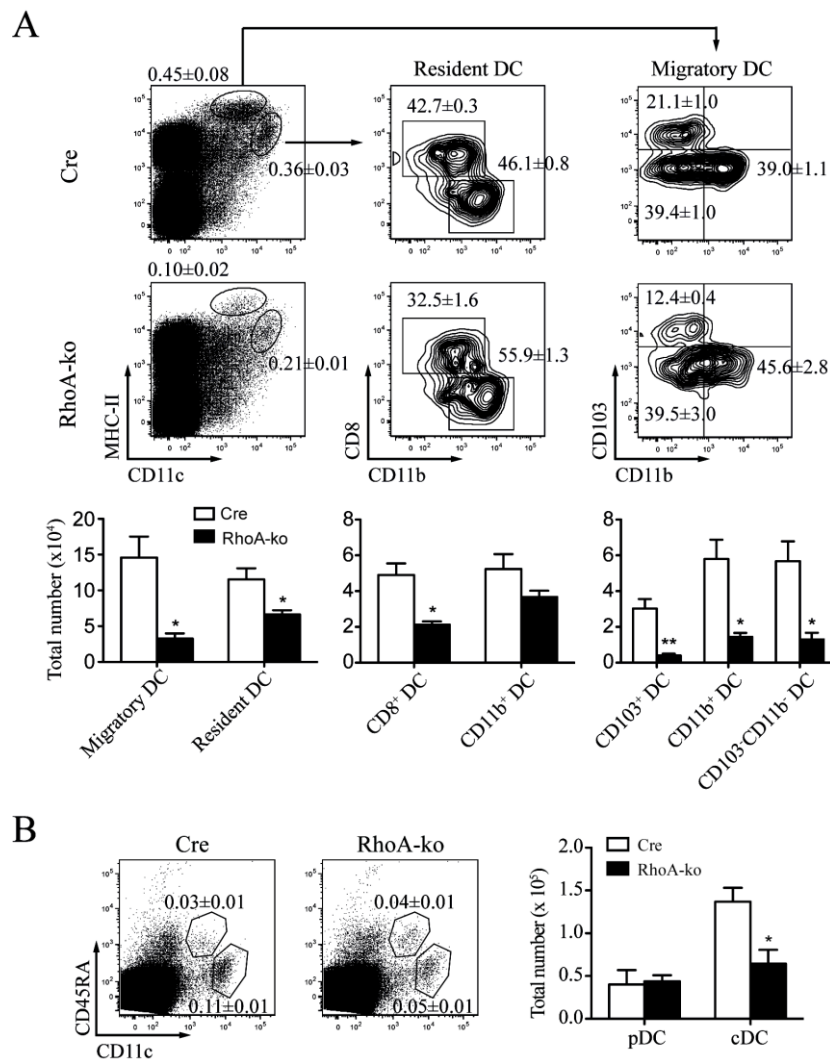
Figure 5. DC reduction in lymph nodes and thymus.
(A) Inguinal, axillary and brachial lymph nodes were pooled and analyzed for DC populations based on expression of CD11c and MHC-II. Resident DCs (MHC-II intermediate) were further analyzed for expression of CD8 and CD11b. Migratory DCs (MHC-II high) were analyzed for expression of CD103 and CD11b.

Percentages represent mean ± SEM (n=3). Bar graphs show the total cell number of DCs and DC subsets in lymph nodes (n=3). (B) pDCs and cDCs were identified as $CD11c^{int}CD45RA^{+}$ and $CD11c^{+}CD45RA^{-}$ respectively in thymus. Total cell number of pDCs and cDCs in thymus were shown in bar graphs (n=3). Figures show representative data of one out of at least three experiments with similar outcome.

5.4 RhoA deletion exclusively affects CD11c^{hi} cells in lymphoid organs

Certain levels of CD11c expression has been found on monocytes, macrophages and activated T cells (Merad et al., 2013). In order to find out if other cells are affected by CD11c-Cre-mediated RhoA deletion, pDCs ($CD45RA^{+}PDCA1^{+}$), monocytes ($Ly6C^{+}CD11b^{+}$), macrophages ($B220^{-}F4/80^{+}$) were analyzed in lymph nodes and spleen. As shown in Figure 6A, monocytes and macrophages were unaltered in lymph nodes and spleens of RhoA-ko mice. Numbers of CD11c^{low} pDCs were reduced to some extent (Fig. 6A). Furthermore, CD4^{+} T cells, CD8^{+} T cells and B cells in spleen were also analyzed by flow cytometry. As shown in Figure 6B, numbers of CD4^{+} T cells and B cells remained unchanged, while CD8^{+} T cells were slightly reduced in numbers (Fig. 6B). It is known that CD8^{+} T cells partially do express CD11c-driven transgenes (Lin et al., 2003). These data indicate that RhoA deficiency mainly causes reduction in the number of cDCs, which express high level of CD11c.
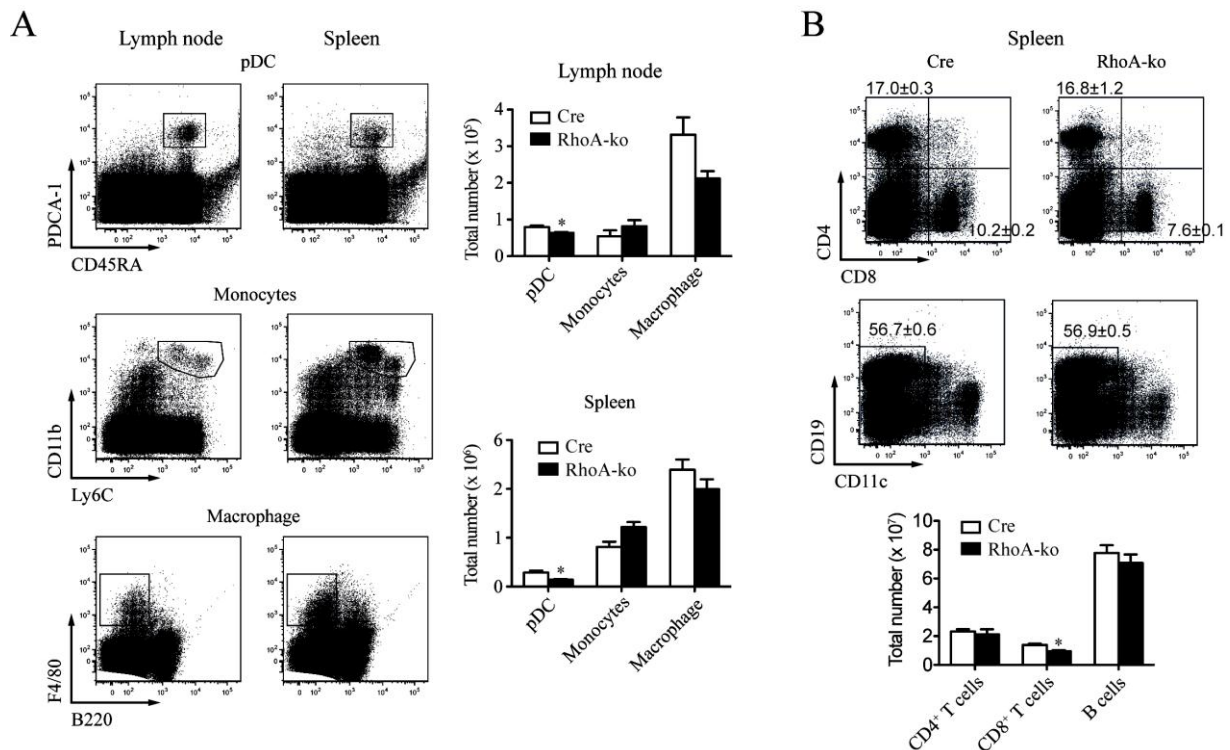
Figure 6. RhoA ko phenotype is restrained in cDCs in lymphoid organs.
(A) pDCs ($PDCA-1^{+}CD45RA^{+}$), monocytes ($CD11b^{+}Ly6c^{+}$) and macrophages ($F4/80^{+}B220^{-}$) were identified in

lymph nodes (as in Fig. 5A) and spleen. The total cell numbers of those cell types were shown in bar graphs (n=3). (B) CD4$^+$ T cells, CD8$^+$ T cells and B cells are identified in the spleen of Cre control and RhoA-ko mice. Bar graphs show total cell numbers of CD4$^+$ T cells, CD8$^+$ T cells and B cells in spleen (n=3). Figures show representative data of one out of at least three experiments with similar outcome.

5.5 RhoA deficiency does not affect the seeding of DC precursors into spleen

cDCs are generated by their immediate precursors called pre-cDCs, which originate from hematopoietic stem cells in the BM (Liu et al., 2009; Naik et al., 2006; Satpathy et al., 2012). To test if the observed DC reduction was caused by defects of pre-cDCs, we analyzed frequencies of pre-cDC in BM and spleen. As shown in Fig. 7A, pre-cDCs are identified as Lin$^-$CD11c$^+$MHC-II$^-$CD43$^+$Sirpα^{int} cells in BM and spleen. Pre-cDCs represent around 0.25% of BM cells and 0.18% of spleen cells (Fig. 7A). RhoA deficiency did not affect the frequency and total number of pre-cDCs in BM and spleen (Fig. 7A). As pre-cDCs express only low levels of CD11c, it was necessary to confirm if RhoA gene has been effectively deleted in RhoA-ko pre-cDCs. A qPCR was performed to examine relative RhoA mRNA transcripts in pre-cDCs. Pre-cDCs from BM still contained normal levels of RhoA mRNA (Fig. 7B). Interestingly, after seeding in spleen, pre-cDCs showed significantly reduced RhoA mRNA (Fig. 7B), suggesting the migration process might provide essential time for deletion of RhoA gene. However, the frequency and total number of pre-cDCs still remained unaffected by RhoA deficiency in spleen (Fig. 7A). These results suggest that RhoA deficiency does not affect the seeding of pre-cDC into spleen.

B
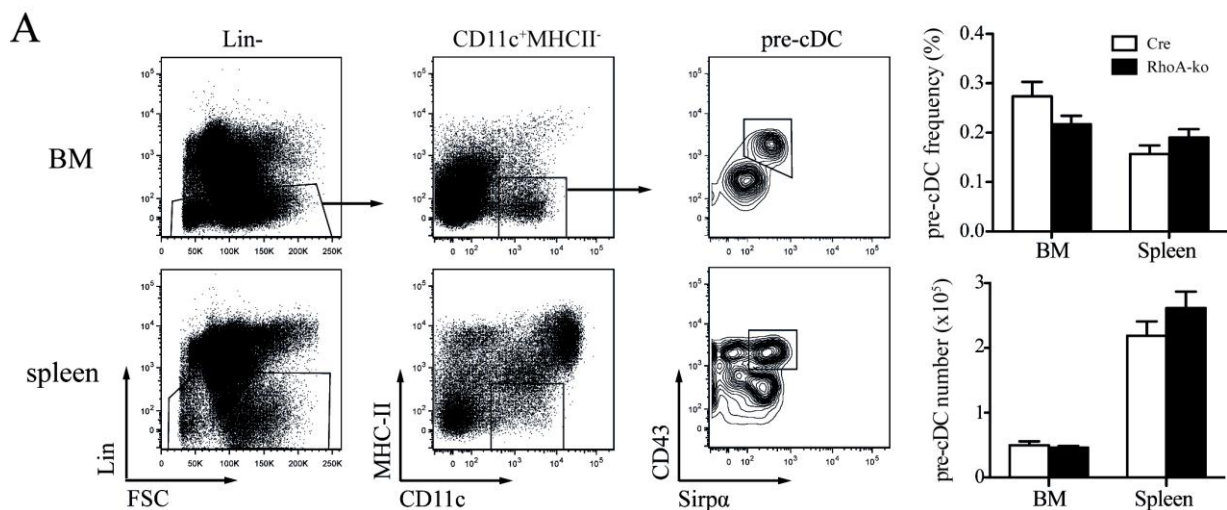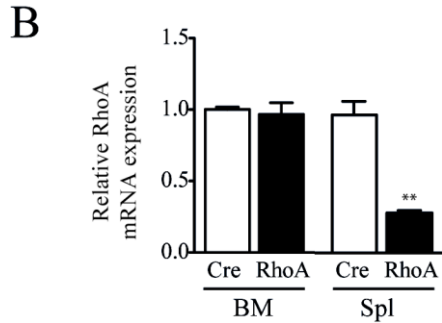
Figure 7. Deletion of RhoA does not affect the seeding of pre-cDCs into spleen
(A) Pre-cDCs are recognized as Lin$^-$CD11c$^+$MHC-II$^-$CD43$^+$Sirpα^{int} in BM and spleen. Bar graphs show the percentages and total numbers of pre-cDCs in BM and spleen (n=3). Lin: CD3/CD19/NK1.1/B220. (B) RhoA mRNA level in pre-cDC was determined by qPCR. Bar graph shows RhoA mRNA transcript in pre-cDCs sorted from BM culture supplemented with Flt3L or directly from spleen (n=3). Figures show representative data of one out of three experiments with similar outcome.

5.6 The generation of cDCs from progenitors is not affected in RhoA-ko mice

Since the frequency and total cell numbers of pre-cDCs are not affected, we further asked if the observed cDC reduction was due to defects in the generation of cDCs from their progenitors in RhoA-ko mice. We next analyzed the potential of DC-precursors generating cDCs *in vitro*. Pro-DC (Lin$^-$CD11c$^-$CD43$^+$Ly6C$^-$, pre-cDC precursors) and pre-cDCs (Lin$^-$CD11c$^+$MHC-II$^-$CD43$^+$Sirpα^{int}) were isolated from BM culture supplemented with Flt3L or directly from spleen as described previously (Naik et al., 2006; Naik et al., 2007), and cultured *in vitro* to monitor their potential of giving rise to cDCs (Fig. 8). Pro-DCs (CD11c$^-$MHC-II$^-$) first develop into CD11c$^+$MHC-II$^-$ pre-cDCs, and then fully differentiate into CD11c$^+$MHC-II$^+$ cDCs (Fig. 8). These *in vitro* culture analyses showed that pro-DCs from BM of RhoA-ko mice were able to differentiate into pre-cDCs and cDCs normally (Fig. 8, upper panels). Pre-cDCs, either isolated from BM or spleen of RhoA-ko mice, could also differentiate normally into cDCs *in vitro* (Fig. 8, lower panels). This result suggests that the generation of cDCs from DC precursors is not affected in RhoA-ko mice (Fig. 8).
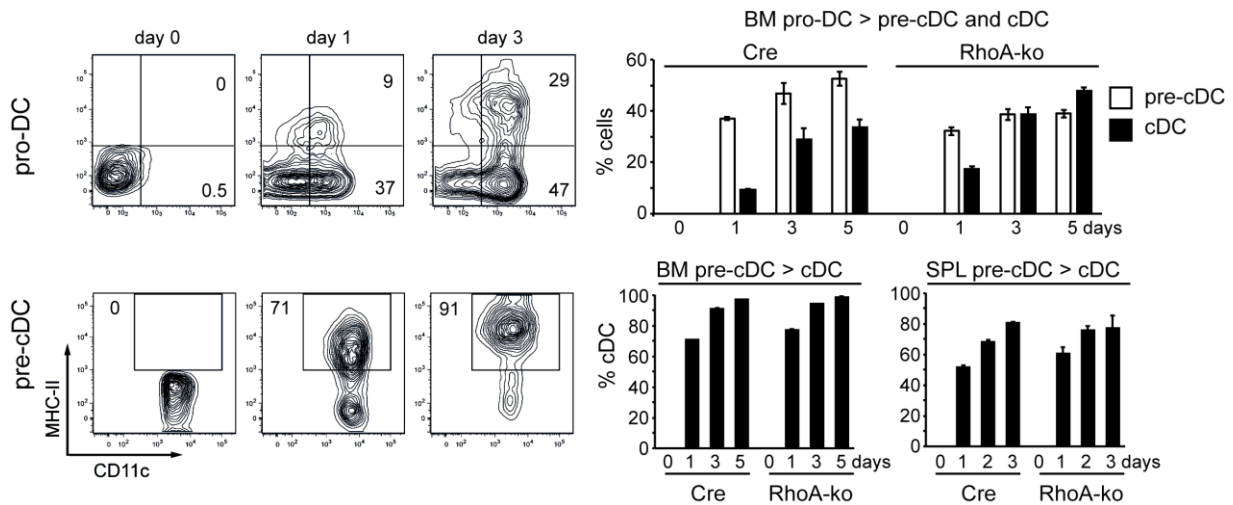
Figure 8. The generation of cDCs from progenitors is not affected in RhoA-ko mice.
Pro-DCs (Lin⁻CD11c⁻CD43⁺Ly6C⁻) and pre-cDCs (Lin⁻CD11c⁺MHC-II⁻CD43⁺Sirpα^int) were sorted from BM culture supplemented with Flt3L; Meanwhile pre-cDCs were also sorted directly from spleen. Then, pro-DCs and pre-cDCs were re-cultured *in vitro* for 3-5 days. The expression of CD11c and MHC-II was monitored over days by flow cytometry. Bar graphs show the generation of pre-cDC or cDC from pro-DC or pre-cDC (n=3). Figures show representative data of one out of three experiments with similar outcome.

5.7 cDC reduction is DC-intrinsic in RhoA-ko mice

To further investigate whether the cDC reduction is a cell intrinsic effect, or rather caused by secondary factors in spleens of RhoA-ko mice, we generated BM-chimeras. To this end, we transferred a 50:50 mixture of CD45.1⁺ CD11c-Cre control and CD45.2⁺ RhoA-ko BM cells was into lethally irradiated CD45.2⁺ B6 mice. As control, we also transferred 100% CD45.1⁺ BM cells into irradiated CD45.2⁺ B6 mice. These mice were analyzed alongside with the experimental groups, and we found less than 1% of total cells derived from host BM, suggesting a near-complete eradication of host BM (data not shown). After 8 weeks, we analyzed DC reconstitution in these mixed BM chimeras. RhoA-deficient cDCs reconstituted only 13% of the cDC-pool in spleens of mixed BM chimeras (Fig. 9A). Compared to CD11c-Cre control, RhoA-deficient CD8⁺ and CD11b⁺Esam^hi DCs were dramatically decreased in total cell number (Fig. 9B). In contrast, CD11b⁺Esam^lo DCs showed only a slight number decrease (Fig. 9B) confirming the normal homeostasis independent of RhoA. Furthermore, expression of CD4 was significantly reduced in RhoA-ko-derived CD11b⁺ cDCs (Fig. 9A), similar as observed in steady state RhoA-ko mice (Fig. 4A). In mixed BM chimeras, a distinct population of CD8⁻CD11b⁻ cDCs became more apparent (Fig. 9A) compared to frequencies in the non-competitive situation (Fig. 4A), which are the natural immature stages of CD8⁺ DC

and $CD11b^+$ (Lewis et al., 2011). However, these RhoA-deficient $CD8^-CD11b^-$ cDCs were also markedly reduced in total numbers compare to Cre controls (Fig. 9B). As internal controls, B and T cells were also analyzed in mixed BM chimeras. RhoA-deficient BM cells generated B and T cells with slightly higher efficiency compared to CD11c-Cre-derived BM cells (Fig. 9B). Taken together, these results indicate that cDC reduction is cell intrinsically due to RhoA deficiency and not caused by secondary effects.
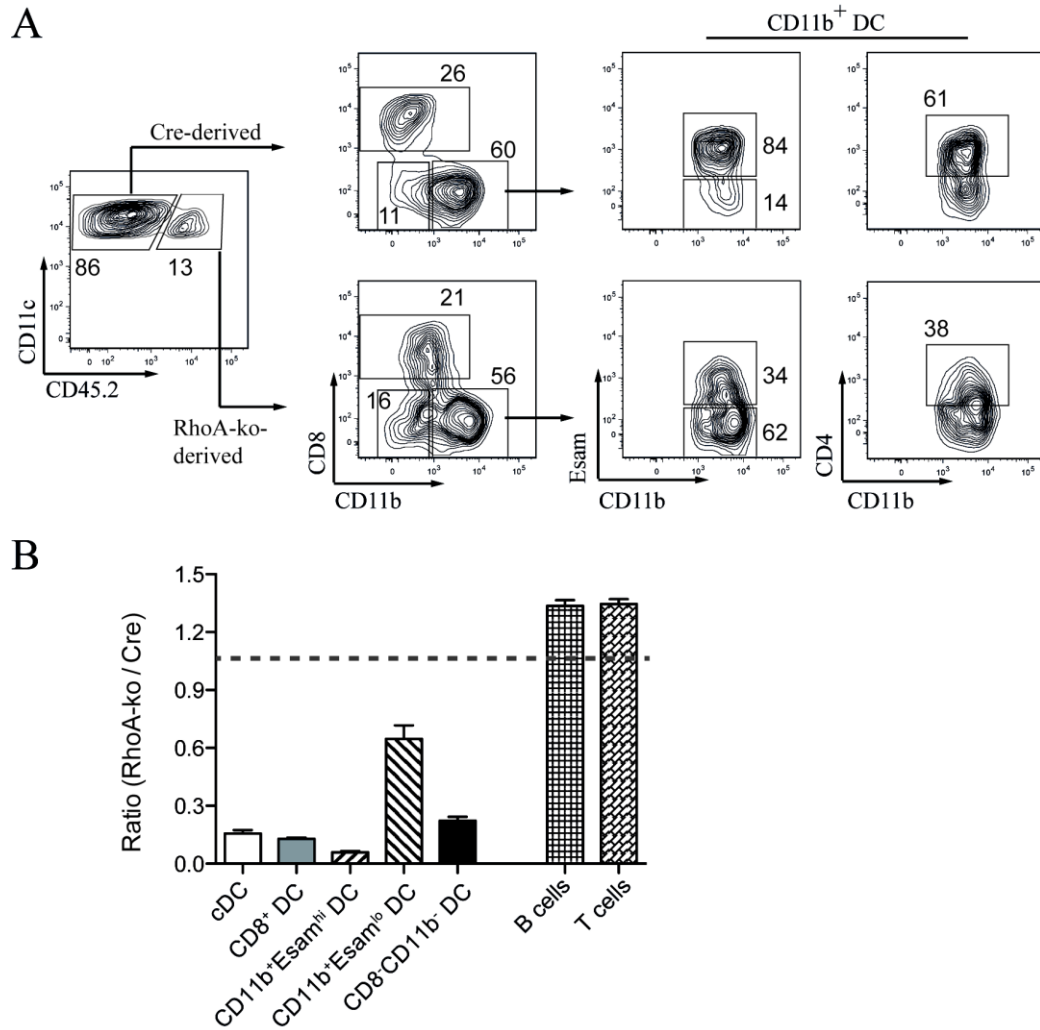
Figure 9. DC reduction caused by RhoA deficiency is cell intrinsic.
(A) Irradiated B6 mice (CD45.2) were reconstituted with a BM mixture equally from CD11c-Cre control (CD45.1) and RhoA-ko (CD45.2) mice. After 8 weeks of reconstitution, cDC and DC subsets were characterized by flow cytometry. Cre-control-derived-cDCs were gated on $CD45.2^-CD11c^+$, while RhoA-ko-derived cDCs were gated on $CD45.2^+CD11c^+$. (B) Bar graph shows the ratio of $CD45.2^+$ RhoA-ko-derived cells vs. $CD45.1^+$ CD11c-Cre-derived cells. The ratio of 1 represents equal contribution of $CD45.1^+$ and $CD45.2^+$ cells. Bars represent mean ± SEM for three mice. Figure shows representative data of one out of four experiments with similar outcome.

5.8 RhoA deficiency indirectly causes increased rate of Ki67^{+} proliferating cDCs in spleen.

DCs were initially thought as non-dividing cells, until recent studies showed that about 5% of cDCs in the spleen were dividing at any time (Kabashima et al., 2005; Liu et al., 2007). Therefore, cDC *in situ* proliferation is very important for maintaining homeostatic cDC numbers in spleen. So we wondered if cDC *in situ* proliferation was affected by RhoA deficiency. In order to test DC proliferation, we stained spleen cDCs with nuclear dye DAPI and an antibody against proliferation marker Ki67 (Fig. 10). As described previously, about 5% of spleen cDCs were proliferating (DAPI[+]Ki67^{+}) in CD11c-Cre control mice (Fig. 10A). However, cDC proliferation rate increased more than two-fold in spleens of RhoA-ko mice (11.7%, Fig. 10A). To determine if this enhanced proliferation was caused by RhoA deficiency, or rather by altered environmental effects, we further analyzed cDC proliferation in mixed BM-chimeras as described above (Fig. 9). In this competitive situation, we were able to analyze proliferation of control- and RhoA-ko-derived cDCs in the same microenvironment. Here, the proliferation rate of RhoA-ko-derived cDCs significantly decreased to around 5% (Fig. 10B), as compared to non-chimeras (Fig. 10A, 11.7%). Both, Cre control- and RhoA-ko-derived cDCs exhibited the same normal proliferation rate, suggesting that the increased cDC proliferation in RhoA-ko mice (Fig. 10A) was not caused by RhoA deficiency itself, but rather by secondary effects. Then we wondered which secondary effects might cause enhanced proliferation of cDCs in spleens of RhoA-ko mice. It has been reported that constitutive ablation of cDC led to significantly elevated serum levels of Flt3L, which in turn caused myeloproliferation (Birnberg et al., 2008). Since Flt3L plays an important role in promoting DC proliferation (Waskow et al., 2008), we therefore measured serum levels of Flt3L. In RhoA-ko mice, serum levels of Flt3L were significantly elevated compared to control mice (Fig. 10C). These findings suggest that RhoA is not required for proliferation of cDCs. However, the reduction of cDC numbers leads to elevated levels of Flt3L in serum, which in turn induces enhanced cDC proliferation in RhoA-ko mice.
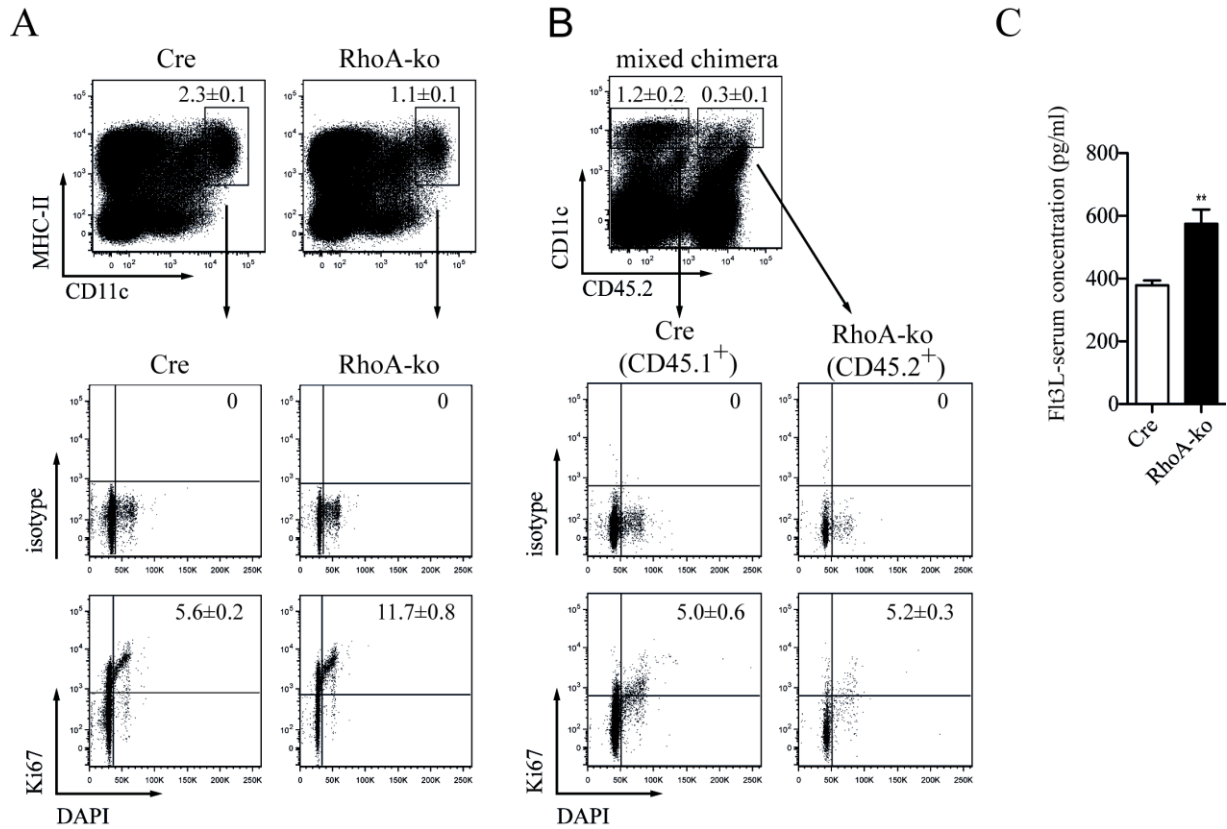
Figure 10. RhoA deficiency causes enhanced proliferation of cDCs due to increased serum Flt3L.
(A) The proliferating cDCs (CD11c$^+$MHC-II$^+$) were detected as Ki67$^+$ in S-G2-M phase (DAPI^{hi}). Isotype antibody was used as negative control for Ki67 staining. The percentages represent mean $\pm$ SEM for three mice. (B) Proliferation rates of Cre-control (CD45.1$^+$) and RhoA-ko (CD45.2$^+$) derived cDCs was measured in 50:50 mixed BM chimeras by flow cytometry. The percentages represent mean $\pm$ SEM for three mice. (C) Serum levels of Flt3L of Cre control and RhoA-ko mice were determined via ELISA (n=6). Figures show representative data from one out of three experiments with similar outcome.

5.9 RhoA controls cytokinesis of DCs

As reported previously, RhoA controls cytokinesis by regulation of cortical contractility and cleavage furrow formation during proliferation (Olson et al., 1995; Sahai and Marshall, 2002). We next examined if RhoA deficiency altered the distribution of DCs at different stages of the cell division cycle (G$_1$, S and G$_2$/M phase). We first analyzed cell cycle in BMDCs and found that RhoA-deficient BMDCs accumulated in S and G$_2$/M-phases (Fig. 11A). In addition, RhoA deficiency caused increased polyploid cells in BMDCs (Fig. 11A). This finding is consistent with previous studies in RhoA deficient keratinocytes (Jackson et al., 2011) and fibroblasts (Melendez et al., 2011). Similarly, spleen cDCs also showed accumulated cells in S and G$_2$/M-phases in RhoA-ko mice, but polynuclear cells *in vivo* were lacking (Fig. 11A).

Furthermore, to test if such accumulation of spleen cDC in S and G_2/M-phases was actually caused by deletion of RhoA or secondary effects, we generated 50:50 mixed BM-chimeras as described above. RhoA-ko-derived cDCs showed an accumulation of cDC in S and G_2/M-phases compared to Cre control (Fig. 11B), indicating a direct effect of RhoA deletion. These data suggest that RhoA regulates cell cycle progression in cDC. To further understand at which phase that RhoA-ko DCs were arrested, we performed mitosis analysis using imagestream (Fig. 11C, D). During mitosis, BMDCs accumulated in the anaphase, while *ex vivo* isolated spleen cDC accumulated in both anaphase and telophase (Fig. 11C), which normally coincide with cytokinesis (Shuster and Burgess, 1999). Taken together, these results suggest that RhoA is critical for regulating cytokinesis in DCs.
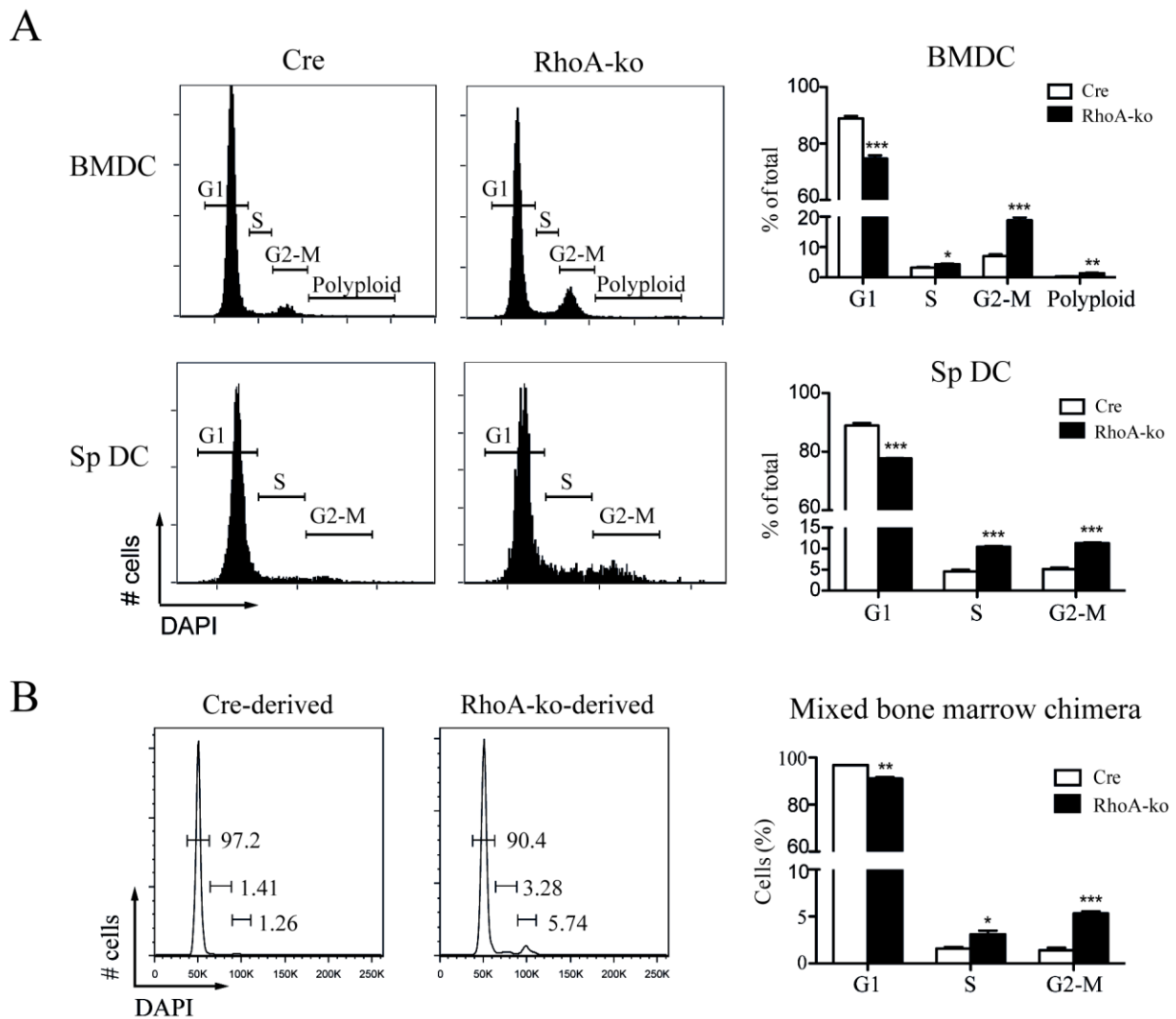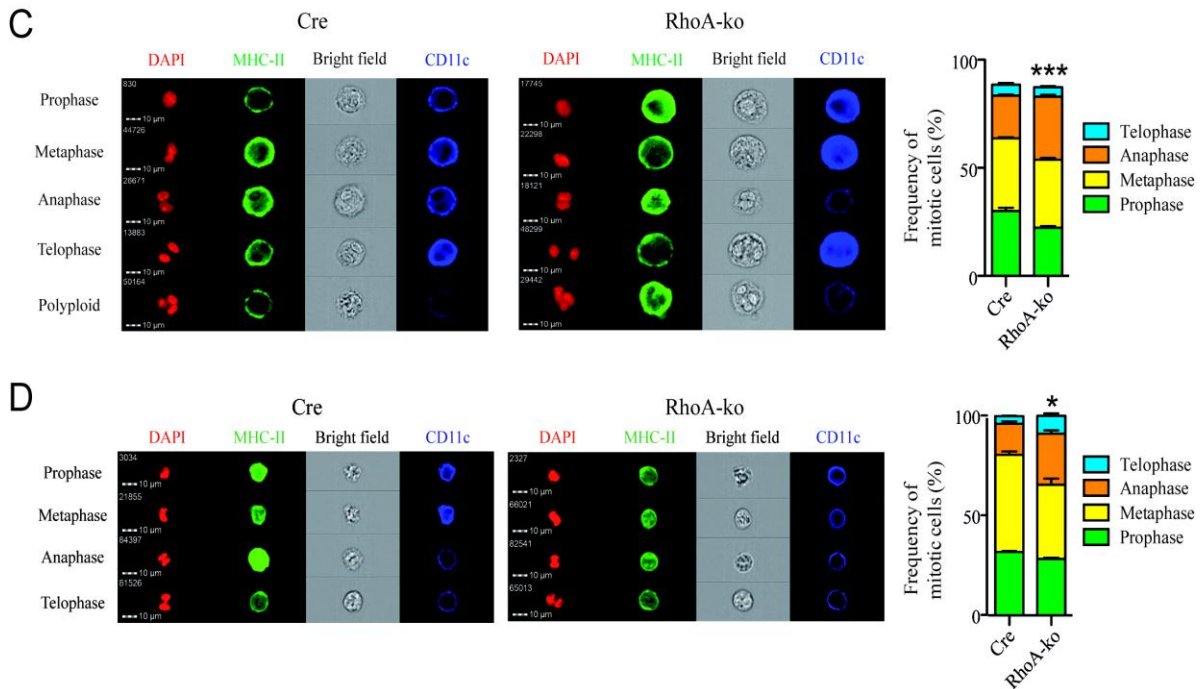
Figure 11. RhoA deficiency causes cytokinesis failure.
(A) Cell cycle of BMDCs and spleen DCs was analyzed by DAPI staining of nuclei. Representative histograms show the cells in different phases (G1, S, G2-M and polyploidy) during cell cycle. Bar graphs indicate the percentages of BMDCs and spleen DCs in different phases (n=3). (B) Cell cycle of spleen DCs in 50:50 mixed BM chimeras was analyzed by flow cytometry. Bar graphs indicate the percentages of cre-control- and RhoA-ko-derived spleen DCs in different phases (n=3). (C) Representative images of BMDCs in different phases of mitosis were selected at random from over 3,000 images by imagestream AMNIS. Bar graph shows the percentages of BMDCs in different phases during mitosis (n=3). (D) Representative images of spleen DCs in different phases of mitosis were selected at random from over 1,000 images. Bar graph shows the percentages of spleen DCs in different phases during mitosis (n=3). Figures show representative data from one out of three experiments with similar outcome.

5.10 RhoA-deficient cDCs show decreased long-term survival

To estimate the influence of RhoA deletion on cDC turnover rates, we performed *in vivo* BrdU pulse-chase experiments (Fig. 12A,B). After three days BrdU pulse, cDCs from RhoA-ko mice exhibited a significant higher BrdU-incorporation rate as compared to cDCs from control mice (Fig. 12A). After withdrawal of BrdU, the percentage of BrdU$^+$ cDCs started to decline over time (Fig. 12A). RhoA-deficient cDCs showed a much faster decline of BrdU-incorporation compared to Cre control (day 9, 12, Fig. 12A). Further analysis of DC subsets showed that both CD8$^+$ and CD11b$^+$ cDCs presented a much faster decline of BrdU-incorporation in RhoA-ko mice (Fig. 12A), suggesting that RhoA-deficient cDCs had a shorter half-life. In order to find out if the reduced cDC turnover rate in RhoA-ko mice is caused

intrinsically by RhoA deletion, we also analyzed cDC turnover in 50:50 mixed BM chimeras (Fig. 12B). In this competitive situation, RhoA-deficient cDCs showed same BrdU-incorporation as Cre control during 3 days pulse phase (Fig. 12B), indicating normal proliferative behavior despite absence of RhoA, which was also determined above by Ki67 staining in mixed BM chimeras (Fig. 10B). Furthermore, RhoA-deficient CD11b$^+$ cDCs showed faster decline of BrdU-incorporation at day 9 and 12, whereas CD8$^+$ cDCs showed faster decline only at day 12 (Fig. 12B), suggesting CD11b$^+$ cDC are more affected by RhoA deficiency than CD8$^+$ cDC. Taken together, these results indicate that RhoA deficiency directly leads to reduced half-life of cDC.
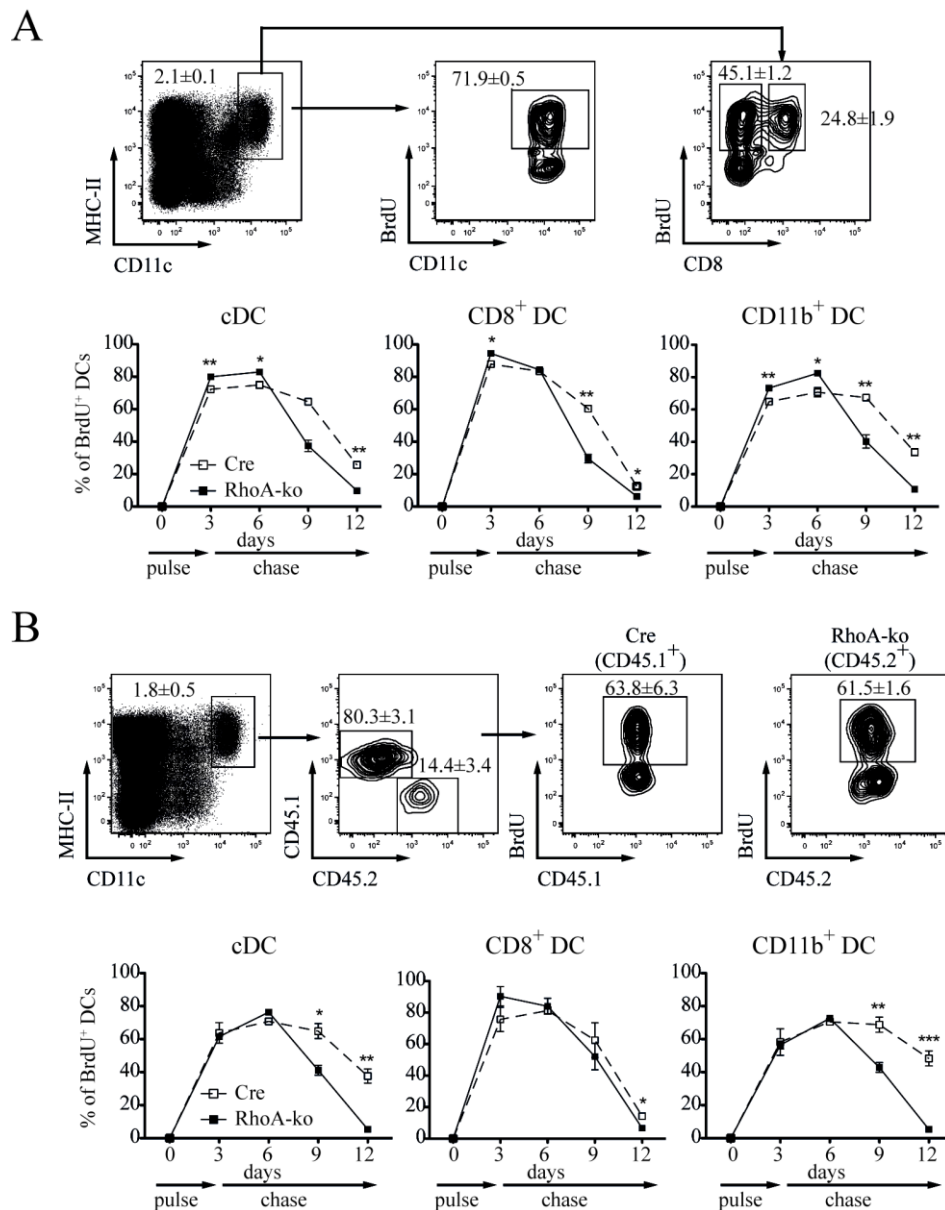
Figure 12. RhoA deficiency results in shorter turnover rate of cDC *in vivo*.
(A) Control and RhoA-ko mice received *in vivo* BrdU-labeling for 3 days (pulse phase), then followed by 9 days of BrdU-free chase phase. The frequency of BrdU$^+$ spleen cDCs, CD8$^+$ and CD11b$^+$ DC subsets was examined by flow cytometry at day 3, 6, 9 and 12. The percentages of BrdU$^+$ DC at each time point within total cDC, CD8$^+$ DC or CD11b$^+$ DC are displayed in line graphs (n=3). (B) 12 days of BrdU pulse-chase experiment was also performed in 50:50 mixed BM chimeras as in fig. 12A (n=3). Line graphs show BrdU kinetics of Cre-control (CD45.1$^+$) and RhoA-ko (CD45.2$^+$) derived total cDCs, CD8$^+$ and CD11b$^+$ cDCs in spleen. Figure shows representative data from one out of 3 experiments with similar outcome.

5.11 RhoA deficiency causes increased apoptosis of cDC

Since BrdU-labeling *in vivo* suggests a shorter half-life in RhoA-deficient cDCs, we next performed TUNEL assays to test if RhoA-deficient cDCs had increased apoptosis in spleen. As shown in Figure 13A (upper panel), RhoA-ko mice exhibited two-fold more TUNEL-positive cDCs in spleen compared to control mice. In addition, we found that most of apoptotic cDCs occurred during G1 phase of cell cycle (DAPI$^-$, Fig. 13A). To confirm that the increased apoptosis is directly due to RhoA-deletion in DCs, we also performed TUNEL assays in mixed BM chimeras. In the competitive situation, RhoA-ko-derived cDCs showed even more severe increased of TUNEL-positive cells, as compared to Cre-control-derived cDCs (Fig. 13A, lower panel), suggesting RhoA intrinsically controlled cDC survival. In order to further confirm that RhoA-deficiency causes increased apoptosis in spleen cDCs, we performed Annexin-V staining combined with viability dye 7-AAD to detect apoptotic spleen cDCs in steady state. Compared to Cre control mice, the percentage of apoptotic CD11b$^+$Esam^{hi} cDCs (Annexin-V$^+$) was significantly increased, while CD8$^+$ and CD11b$^+$Esam^{lo} cDCs did not show significant alteration in RhoA-ko mice (Fig. 13B). As controls we also analyzed Annexin-V positive MHC-II$^+$CD11c$^-$ cells (including B cells) and CD8$^+$CD11c$^-$ cells (including CD8$^+$ T cells), which did not show increased apoptotic cells (Fig. 13B). Furthermore, we also monitored BMDC survival *in vitro* by removing DC growth factor GM-CSF. Upon GM-CSF removal, RhoA-deficient BMDCs showed significantly impaired survival kinetics compared to Cre control (Fig. 13C), which was consistent with *in vivo* findings (Fig. 13A, B). These results indicate that RhoA is essential for maintaining the cDC-survival.
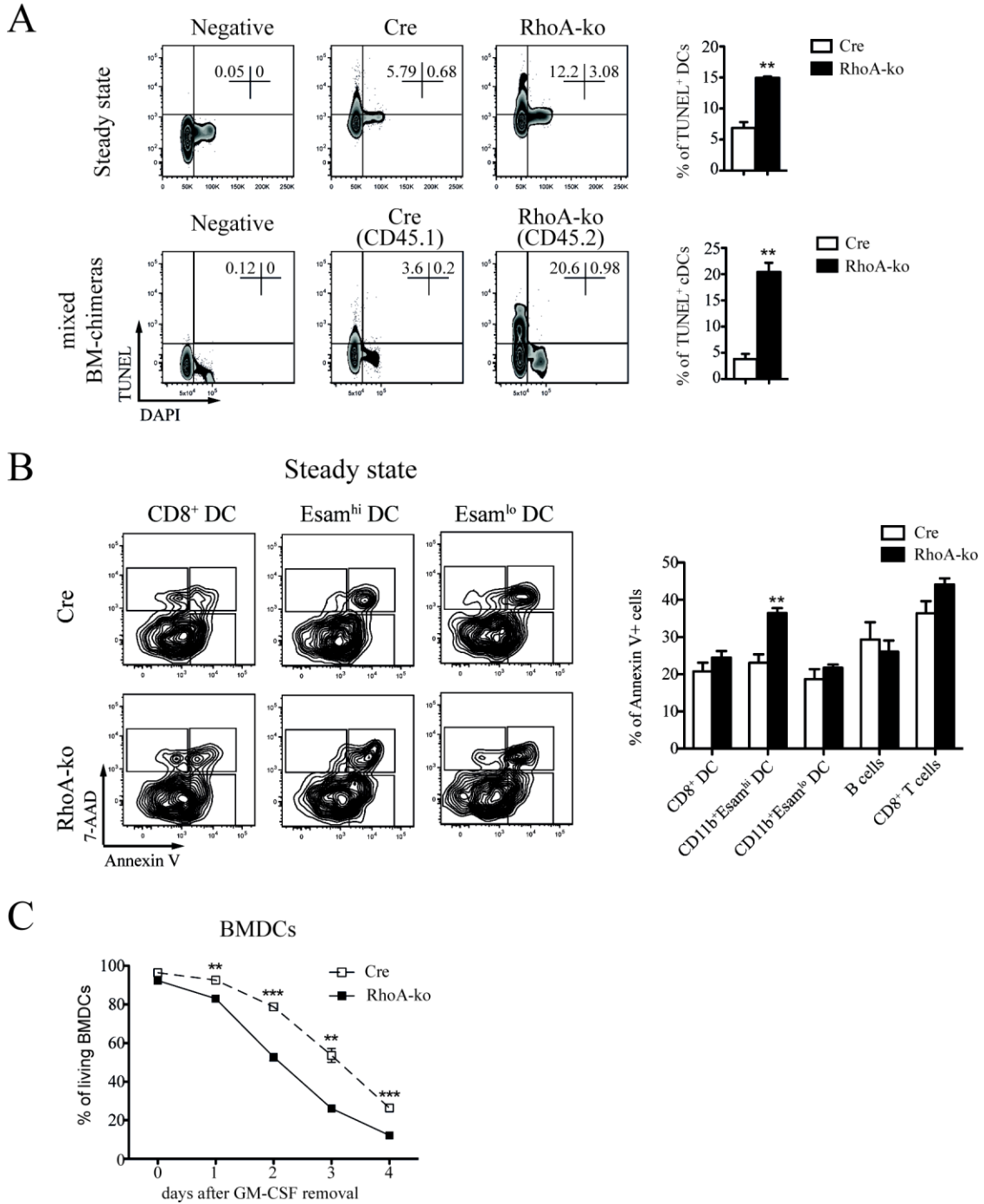
Figure 13. RhoA deficiency leads to increased apoptotic DCs *in vivo* and *in vitro*.
(A) cDCs were first gated on CD11c$^+$MHC-II$^+$ in spleen, then apoptotic cDCs were detected by TUNEL assay in steady state and mixed BM chimeras. Cells were not treated with TdT enzyme as negative control. Combined with DAPI staining, apoptotic cDCs in different stages of cell cycle can be identified. Bar graphs show percentages of total TUNEL$^+$ cDCs in spleen (n=3). (B) Annexin-V and 7-AAD were used for detecting apoptotic CD8$^+$, Esam^{hi} and Esam^{lo} DC subsets in spleens of Cre control and RhoA-ko mice in steady state. Bar graph shows the percentages of total Annexin-V$^+$ DC subsets as well as B cells and CD8$^+$ T cells (n=3). (C) BMDC survival kinetic was monitored over 4 days after removal of GM-CSF (n=3). Figure shows representative data from one out of 3 experiments with similar outcome.

5.12 Proteome analysis of RhoA-deficient DCs

As we already know that RhoA controls cDC-survival based on the results above, and wondered which signaling pathway was involved in RhoA-regulated cDC survival. Therefore, a proteome analysis was performed in collaboration with Stephan Lichtenthaler's group at the German Center for Neurodegenerative Diseases (DZNE) to investigate proteins that were differentially expressed between Cre-control and RhoA-ko BMDCs. Dr. Bastian Dislich (DZNE) performed the protein analysis as well as bioinformatics. A total of 2699 proteins could be identified with at least 2 unique peptides for each protein (Fig. 14A). Only the proteins with more than 3 fold changes are considered as significantly up- or down-regulated in RhoA-ko BMDCs. Therefore, we identified 54 up-regulated and 39 down-regulated proteins, which are listed in table 3 (7. Appendix). According to Gene Ontology (GO) terms, some of those protein play roles in regulating cell cycle progression (GO:0022402) and programmed cell death (GO:0043067), which are displayed as green and red respectively in volcano plots (Fig. 14A). Among those, a pro-survival protein phophoinositide 3-kinase gamma (PI3Kγ) was markedly down-regulated in RhoA-deficient BMDCs (Fig. 14A). Previous studies have shown that PI3Kγ can promote cell survival through phosphorylation of its downstream effector Akt (Comerford et al., 2012; Johnson et al., 2007). Active Akt inhibits the pro-apoptotic function of *Bcl-2*-associated death promoter (*BAD*) by phosphorylating (She et al., 2005). Therefore, we hypothesized that RhoA deletion caused down-regulated PI3Kγ, which in turn led to increased apoptosis due to inefficient phosphorylation of Akt and BAD in DCs. To prove our hypothesis, we performed Western blot to determine protein levels of PI3Kγ, Akt and BAD, as well as phosphorylation of Akt and BAD in BMDCs and spleen cDCs isolated by MACS. First, we verified that RhoA protein has been effectively knocked out in both RhoA-ko BMDCs and spleen cDCs (Fig. 14B). Western blot data showed that PI3Kγ were significantly reduced in both RhoA-ko BMDCs and spleen cDCs (Fig. 14B), confirming the proteomics data. The total protein levels of Akt and BAD remained same between Cre control and RhoA-ko (Fig. 14B). However, phosphorylation of Akt and BAD significantly impaired in RhoA-ko BMDCs and spleen cDCs, possibly due to down-regulation of PI3Kγ. These results indicate that the pro-survival PI3Kγ/Akt/BAD signaling pathway is inhibited in RhoA-deficient DCs, which might be responsible for the increased cDC apoptosis. In addition, to better understand how RhoA regulates the expression of PI3Kγ, we also

analyzed transcripts of PI3Kγ in cDCs. And we found that mRNA levels of PI3Kγ were significantly decreased in RhoA-ko cDCs (Fig14. C), suggesting RhoA might regulate the transcription of PI3Kγ in DCs. Therefore, deletion of RhoA leads to reduced PI3Kγ mRNA transcription, which then results in reduced protein levels of PI3Kγ. However, the exact mechanism how RhoA controls expression of PI3Kγ is still unknown.

It has been reported that RhoA deletion caused increase of HPCs death through programmed necrosis, characterized by up-regulated transcription of necrosis-related genes (Zhou et al., 2013). In order clarify if increased cDC cell death in RhoA-ko mice is rather caused by apoptosis or necrosis, we analyzed mRNA levels of some critical necrosis-induced genes in spleen cDCs, such as tumor necrosis factor alpha (TNF-α), TNFR1, Ripk1, Ripk3, Fth1 and Glud1 (Vandenabeele et al., 2010; Zhou et al., 2013). Compared to Cre control, none of those genes showed significant alteration, except TNF-α, which was rather down-regulated in RhoA-ko spleen cDCs (Fig. 14D). This result suggests that increased cDC death due to RhoA deficiency is not caused by necrosis. Taken together, our findings indicate that RhoA maintains cDC survival through regulating PI3Kγ/Akt/BAD signaling pathway (Fig. 14E).
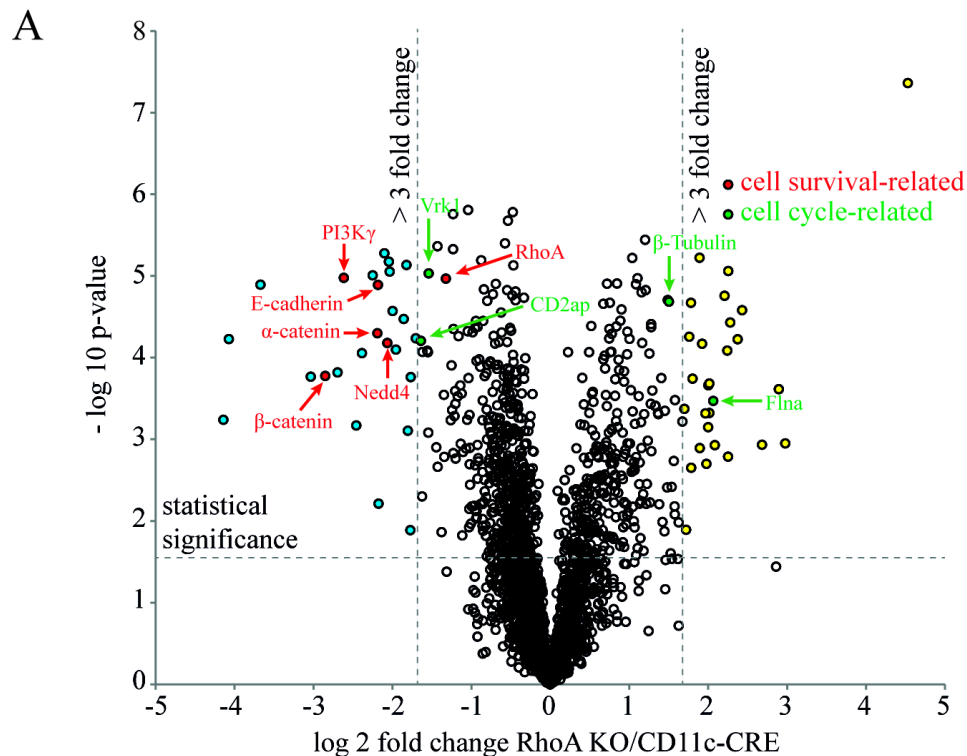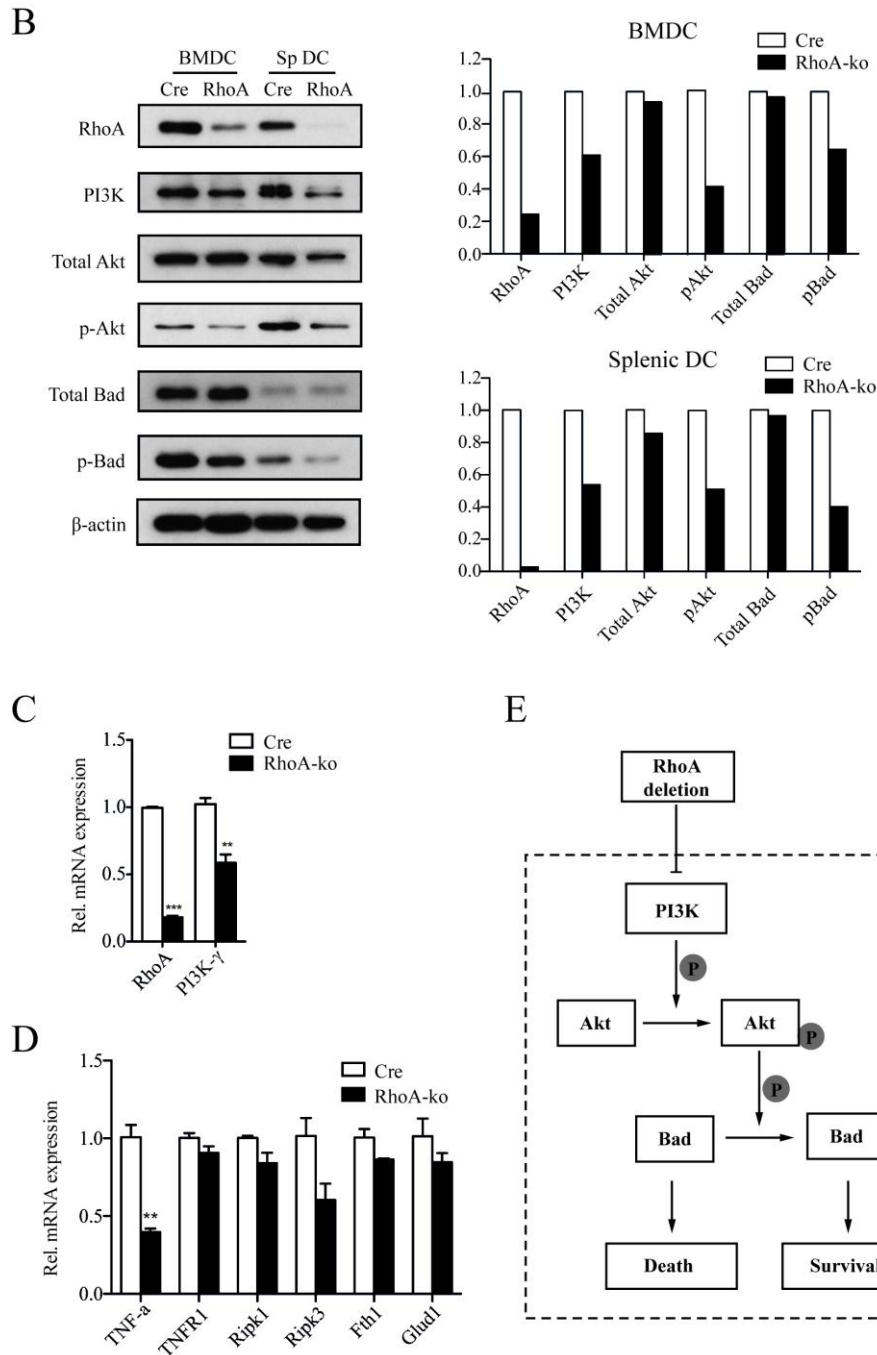
Figure 14. RhoA promotes DC survival through PI3K/Akt/BAD pathway.
(A) BMDCs from Cre control and RhoA-ko mice were used for proteome analysis. A total of 2699 proteins were detected as shown in volcano plots. Proteins that are up- or down-regulated more than 3 fold in the RhoA-ko BMDCs are considered as significantly altered. Among those proteins, cell survival-related proteins (red color) and cell cycle-related proteins (green color) are indicated. (B) The total amount of PI3Kγ, Akt and BAD, as well as phosphorylation of Akt and BAD was determined by Western blot. Bar graphs show quantification of Western blot bands done by ImageJ software. (C) The mRNA of PI3Kγ was determined in spleen cDCs by qPCR. (D) The mRNA of necrosis-related genes in spleen cDCs was determined by qPCR. (E) Sketch of RhoA/PI3K/Akt/BAD signaling pathway regulating DC survival. RhoA-deletion caused down-regulation of PI3Kγ, and inefficient phosphorylation of Akt and BAD resulting in cDC apoptosis.

6. DISCUSSION

6.1 RhoA and DC homeostasis

RhoA, Cdc42 and Rac1 are the best-studied members in small Rho GTPase family, which regulate multiple cell functions including cytoskeleton organization, migration, survival and gene expression (Jaffe and Hall, 2005; Tybulewicz and Henderson, 2009). Previous studies have shown that RhoA plays important roles in regulating morphology, antigen presentation and migration of DCs, by applying C3 transferase, overexpression of dominant-negative mutants or inhibiting the RhoA activator Arhgef5 (Kobayashi et al., 2001; Shurin et al., 2005; Wang et al., 2009). Furthermore, studies using SWAP-70 (an activator of RhoA) deficient mice have indirectly shown that RhoA regulated motility and endocytosis of DCs (Ocana-Morgner et al., 2011), as well as the surface localization of MHC-II in DCs (Ocana-Morgner et al., 2009). However, RhoA functions in DCs are still largely unknown. In this study, we used DC-specific RhoA-ko mouse model to study RhoA functions in DCs, and found that RhoA was crucial for maintaining a defined numbers of cDCs *in vivo* through promoting DC survival.

DCs play a crucial role in regulating both immunity and tolerance *in vivo*. Therefore, it is important to understand how DC homeostasis is maintained in lymphoid organs. The following mechanisms are involved in maintaining suitable numbers of cDCs in lymphoid organs: constant replenishment by precursors, *in situ* proliferation and apoptosis (Liu et al., 2007). RhoA deficiency caused dramatic reduction in number of total cDCs in lymph nodes, spleen and thymus (Fig. 4A, Fig. 5A,B). In spleen, $CD8^+$ DCs and $CD11b^+Esam^{hi}$ DCs were significantly decreased in total cell number, whereas $CD11b^+Esam^{lo}$ DCs largely remained unaltered (Fig. 4B). Unlike other DC subsets, which are derived from pre-cDCs, $CD11b^+Esam^{lo}$ DCs are most likely derived from monocytes or earlier monocytic precursors (Klebanoff et al., 2013; Lewis et al., 2011). Therefore, we speculated that $CD11b^+Esam^{lo}$ DCs probably received constant replenishment from monocytes or some earlier monocytic precursors, which compensated the loss of this DC subset in steady state. However, the precise origin of $CD11b^+Esam^{lo}$ DCs is still unknown, and needs to be defined.

6.2 RhoA and DC proliferation

It has been reported earlier that inhibition of RhoA caused impaired proliferation of breast cancer cells (Pille et al., 2005). So we wondered if RhoA deficiency caused impaired proliferation of DC, which could lead to cDC reduction. In contrast, we found that the rate of proliferating cDCs was not impaired, but rather increased more than two-fold in spleens of RhoA-ko mice, compared to Cre control mice (Fig. 10A). However, further analysis in mixed BM chimeric mice showed that RhoA-deficient cDCs had the same proliferation rate of 5% as Cre-control cDCs (Fig. 10B), suggesting that the enhanced DC proliferation in RhoA-ko mice was rather caused by environmental factors, but not directly related to RhoA-deletion. To find out which environmental factors altered in RhoA-ko mice causing enhanced cDC proliferation, we first analyzed Flt3L. Its receptor, Flt3, is expressed on DCs, but not on other cells such as B cells, T cells, NK cells and monocytes (Karsunky et al., 2003). Therefore, cDCs are considered as major "consumers" of Flt3L among peripheral mature hematopoietic cells (Karsunky et al., 2003). Loss of cDC might cause accumulation of Flt3L, resulting in abnormally high concentrations of this growth factor, which in turn might trigger increased cDC proliferation (Karsunky et al., 2003). In the CD11c-DTR mouse model, complete ablation of cDC led to a 3-fold increase of Flt3L in serum and enhanced proliferation *in vivo* (Birnberg et al., 2008). In RhoA-ko mice, the numbers of cDC were reduced around 2-fold in spleens, leading to 1.5-fold increased Flt3 serum-concentration (Fig. 10C). The increased levels of Flt3L promoted cDC proliferation, which to some extent compensated the loss of cDCs caused by RhoA deletion. This increased proliferation was abrogated in mixed BM-chimeras, where competitor wt DCs could fill up the DC-pool to normal numbers. This data suggest that altered numbers of cDCs change the balance of environmental effectors such as Flt3L, which in turn affects cDC proliferation. Similarly, RhoA deficiency in HSC also led to significant increase in proliferation of HSCs, which might be a secondary effect due to acute hematopoietic stress (Zhou et al., 2013). In addition, it has been shown that B cell proliferation was not affected by RhoA deletion by using a B cell specific RhoA-ko mouse model (Zhang et al., 2012). Taken together, our data indicate that RhoA is dispensable for proliferation of DC, but deletion of RhoA leads to enhanced proliferation of cDC due to elevated Flt3L.

6.3 RhoA and DC survival

Previous studies have shown that RhoA plays a crucial role in promoting cell survival (Hippenstiel et al., 2002; Reuveny et al., 2004; Zhu et al., 2008). We therefore studied DC apoptosis, and found significant increased TUNEL and Annexin-V positive cDCs in RhoA-ko mice (Fig. 13A,B). In addition, we observed significantly increased DCs accumulating in G2-M phase of the cell cycle (Fig. 11A). Imagestream analysis showed that RhoA-deficient cDCs were arrested in anaphase and telophase during mitosis (Fig. 11C,D). It has been reported that RhoA is critical for regulating cleavage furrow formation and separation of two daughter cells during mitosis, deletion of which would lead to increased multi-nucleated cells (Geddis et al., 2007; Lordier et al., 2008). Mitotic failure results in polyploid cells, which may trigger cell death (Castedo et al., 2004). Therefore, the observed mitotic failure in cDCs due to RhoA deficiency might lead to DC death. Recently, a pro-apoptosis protein BAD has been identified to contribute to mitotic cell death in mitochondrial apoptosis pathway (Diaz-Martinez et al., 2014). The phosphorylation of BAD was clearly inhibited in RhoA-ko cDCs, which may be linked to mitotic cell death through the mitochondrial apoptosis pathway. However, it is still unclear if the increased apoptosis in RhoA-ko cDCs is caused by mitotic failure. Further work is required to find the correlation between mitotic failure and DC apoptosis.

Our proteome analysis showed a pro-survival protein PI3Kγ significantly down-regulated in RhoA-deficient DCs. Previous studies have shown that deletion of PI3Kγ led to increased apoptosis of leukocytes (Rodrigues et al., 2010) and CD4^{+} T cells (Comerford et al., 2012) by using PI3Kγ-deficient mice. Furthermore, PI3Kγ-deficiency also caused significant decrease of cDCs in spleen (Del Prete et al., 2004), as well as death of migratory DCs in dLNs (Comerford et al., 2012). These DC reductions in PI3Kγ-deficient mice are quite consistent with our findings in RhoA-ko mice (Fig. 4A and Fig. 5A), suggesting PI3Kγ might play an important role in RhoA-regulated DC homeostasis. In RhoA-deficient DCs, the expression of PI3Kγ was strongly reduced, which led to inefficient phosphorylation and activation of its downstream effector Akt (Fig. 14B). Therefore, the pro-apoptotic protein BAD, a downstream target of Akt, cannot be effectively inactivated through phosphorylation. Consequently, more apoptosis was induced in RhoA-ko DC. However the mechanism of how RhoA regulates the expression of PI3Kγ in DC is still unclear. But we also found that RhoA deletion caused

significantly reduced transcription of PI3Kγ mRNA in spleen cDCs (Fig. 14C), suggesting a transcriptional regulation by RhoA. Previous studies have revealed that RhoA regulated gene transcriptions via modulating transcription factor GATA-4 (Charron et al., 2001) and the c-fos serum response element (SRE) (Hill et al., 1995). However, it is still unknown which transcription factors were utilized by RhoA to regulate expression of PI3Kγ in DCs. Therefore further analysis is required to investigate the mechanism of how RhoA regulates PI3Kγ/Akt/BAD pro-survival signaling pathway. Furthermore, other studies showed receptors for GM-CSF (Kohno et al., 2004; Muessel et al., 2008) and Flt3L (Mali et al., 2011) regulated cell migration and survival through RhoA signaling. Therefore, RhoA might act as a sensor of GM-CSF and Flt3L to promote DC survival, through regulating PI3Kγ/Akt/BAD signaling pathway.

In summary, our findings revealed a crucial role for RhoA in regulating the homeostasis of cDCs in spleen. RhoA-deficient cDCs exhibited clearly increased apoptosis, resulting in significantly reduced numbers of cDCs in spleen. Proteome analysis suggests that RhoA maintains DC survival via PI3Kγ/Akt/BAD signaling pathway.

7. APPENDIX

7.1 Proteomics data

54 proteins were up-, and 39 proteins were down-regulated more than 3-fold in RhoA-deficient BMDCs. These proteins are listed in the following table in the order of fold changes. With the help of Dr Stephan Müller (DZNE), the proteomics data have been deposited to the ProteomeXchange Consortium (Vizcaino et al., 2014) (www.proteomexchange.org) via the PRIDE partner repository with the dataset identifier PXD001636 (Username: reviewer17494@ebi.ac.uk; Password: FYSzY7vG).

Table 3: Proteins differentially expressed between wt and RhoA-ko BMDCs.

Gene Name	Protein Name	Fold change (RhoA-ko/Wt)
Up-regulated (>3 fold)		
Vps13c	Vacuolar protein sorting-associated protein 13C	23
Lrp1	Low-density lipoprotein receptor-related protein 1	8
Serpinb2	Plasminogen activator inhibitor 2, macrophage	7
Selenbp1;2	Selenium-binding protein 1;2	7
Mrc1	Macrophage mannose receptor 1	6
Ctsd	Cathepsin D	5
Ctsb	Cathepsin B	5
Lrpap1	Alpha-2-macroglobulin receptor-associated protein	5
Myof	Myoferlin	5
Lamp1	Lysosome-associated membrane glycoprotein 1	5
Ephx1	Epoxide hydrolase 1	5
Gpnmb	Transmembrane glycoprotein NMB	5
Pls3	Plastin-3	4
Anxa3	Annexin A3	4
Vat1	Synaptic vesicle membrane protein VAT-1 homolog	4

Flna	Filamin-A	4
Lyz2	Lysozyme C-2	4
Cd36	Platelet glycoprotein 4	4
Mgll	Monoglyceride lipase	4
Gda	Guanine deaminase	4
Atp6v0d2	V-type proton ATPase subunit d 2	4
Lpl	Lipoprotein lipase	4
Fabp5	Fatty acid-binding protein, epidermal	4
Idh1	Isocitrate dehydrogenase [NADP]	3
Il1rn	Interleukin-1 receptor antagonist protein	3
Msr1	Macrophage scavenger receptor types I and II	3
Asph	Aspartyl/asparaginyl beta-hydroxylase	3
Ahnak2		3
Hmox1	Heme oxygenase 1	3
Blvrb	Flavin reductase (NADPH)	3
Gla	Alpha-galactosidase A	3
Aldh1a2	Retinal dehydrogenase 2	3
Car4	Carbonic anhydrase 4	3
Prdx5	Peroxiredoxin-5, mitochondrial	3
Ddhd1	Phospholipase DDHD1	3
Papss2	Sulfate adenylyltransferase	3
Tmem106a	Transmembrane protein 106A	3
Nudt16	U8 snoRNA-decapping enzyme	3
Stom	Erythrocyte band 7 integral membrane protein	3
Ctsl1	Cathepsin L1	3
Tubb2a;Tubb2b	Tubulin beta-2A chain;Tubulin beta-2B chain	3
Dusp3	Dual specificity protein phosphatase 3	3
Ass1	Argininosuccinate synthase	3

Aldh1l1	Cytosolic 10-formyltetrahydrofolate dehydrogenase	3
Fabp4	Fatty acid-binding protein, adipocyte	3
Lgals3bp	Galectin-3-binding protein	3
Gstm2	Glutathione S-transferase Mu 2	3
Lgmn	Legumain	3
Ptgr1	Prostaglandin reductase 1	3
Pfkl	6-phosphofructokinase, liver type	3
Gstm1	Glutathione S-transferase Mu 1	3
Ctsz	Cathepsin Z	3
Adssl1	Adenylosuccinate synthetase isozyme 1	3
Ddx58	Probable ATP-dependent RNA helicase DDX58	3

Gene Name	Protein Name	Fold change (RhoA-ko/Wt)
Down-regulated (>3 fold)		
Alox12l	Arachidonate 12-lipoxygenase, leukocyte-type	-18
Avil	Advillin	-17
Gbp2	Interferon-induced guanylate-binding protein 2	-13
	MLV-related proviral Env polyprotein	-8
Ctnnb1	Catenin beta-1	-7
Card9		-6
Pik3cg	Phosphatidylinositol 4,5-bisphosphate 3-kinase gamma	-6
Lacc1	Laccase domain-containing protein 1	-5
Trp53i11	Tumor protein p53-inducible protein 11	-5
Rtn1	Reticulon-1	-5
Ctnna1	Catenin alpha-1	-5
Cdh1	Cadherin-1	-5
Scin	Adseverin	-5

Aif1	Allograft inflammatory factor 1	-4
Nedd4	E3 ubiquitin-protein ligase NEDD4	-4
Lipe	Hormone-sensitive lipase	-4
Ttc39b	Tetratricopeptide repeat protein 39B	-4
L1cam	Neural cell adhesion molecule L1	-4
Pram1	PML-RARA-regulated adapter molecule 1	-4
Tfrc	Transferrin receptor protein 1	-4
Pgm2l1	Glucose 1,6-bisphosphate synthase	-4
Grap2	GRB2-related adaptor protein 2	-3
Kmo	Kynurenine 3-monooxygenase	-3
Dok3	Docking protein 3	-3
Tppp3	Tubulin polymerization-promoting protein 3	-3
Cd2ap	CD2-associated protein	-3
Mfge8	Lactadherin	-3
Glb1	Beta-galactosidase	-3
Enah	Protein enabled homolog	-3
2010005H15Rik		-3
Bckdha	2-oxoisovalerate dehydrogenase subunit alpha	-3
Vrk1	Serine/threonine-protein kinase VRK1	-3
Cst3	Cystatin-C	-3
H2-Eb1	H-2 class II histocompatibility antigen	-3
Hsd17b4	Peroxisomal multifunctional enzyme type 2	-3
Plet1	Placenta-expressed transcript 1 protein	-3
H2-Aa	H-2 class II histocompatibility antigen, A-B alpha chain	-3
Spn	Leukosialin	-3
RhoA	RhoA	-3

8. ABBREVIATIONS

ACK	Ammonium chloride potassium
APC	Antigen presenting cell
APC	Allophycocyanin
BM	Bone marrow
BMDC	Bone marrow derived dendritic cells
bp	Base pair
BrdU	Bromodeoxyuridine
CD	Cluster of differentiation
cDC	Conventional dendritic cell
cDNA	Complementary DNA
CSF1R	Colony stimulating factor 1 receptor
CTL	Cytotoxic T lymphocyte
CXCL	C-X-C motif chemokine ligand
CXCR	C-X-C motif chemokine receptor
DC	Dendritic cell
dLN	Draining lymph node
ELISA	Enzyme-linked immunosorbent assay
FACS	Fluorescence activated cell sorter
FCS	Fetal calf serum
FITC	Fluoresceinisothiocyanate
Flt3L	FMS-like-tyrosine-kinase 3 ligand
IFN	Interferon
GAP	GTPase activating protein

GDI	Guanine nucleotide dissociation factor
GDP	Guanosine diphosphate
GEF	Guanine nucleotide exchange factor
GM-CSF	Granulocyte macrophage colony-stimulating factor
GTP	Guanosine triphosphate
HPCs	Hematopoietic progenitor cells
HPRT	Hypoxanthine phosphoribosyltransferase
i.p. / i.v.	Intraperitoneal / intravenous
IL	Interleukin
KO	Knockout
LN	Lymph node
LTβR	Lymphotoxin-β receptor
MACS	Magnetic cell sorting
mg, ml, mM, M	Milligram, Milliliter, Millimolar, Molar
min	Minutes
mRNA	Messenger RNA
PBS	Phosphate buffered saline
PCR	Polymerase chain reaction
pDC	Plasmacytoid DC
PE	Phycoerythrin
PerCP	Peridinin-Chlophyll
pH	Power of hydrogen
qPCR	Quantitative PCR
RA	Recnoic acid

RT	Room temperature
SDS	Sodium dodecyl sulfate
TAE	Tris-acetate-EDTA buffer
TEMED	Tetramethylethylenediamine
TUNEL	TdT-mediated dUTP-biotin nick end labeling
WT	Wild type
μg, μl, μm	Microgram, Microliter, Micrometer

9. REFERENCES

Birnberg, T., Bar-On, L., Sapoznikov, A., Caton, M.L., Cervantes-Barragan, L., Makia, D., Krauthgamer, R., Brenner, O., Ludewig, B., Brockschnieder, D.*, et al.* (2008). Lack of conventional dendritic cells is compatible with normal development and T cell homeostasis, but causes myeloid proliferative syndrome. Immunity *29*, 986-997.

Bogunovic, M., Ginhoux, F., Helft, J., Shang, L., Hashimoto, D., Greter, M., Liu, K., Jakubzick, C., Ingersoll, M.A., Leboeuf, M.*, et al.* (2009). Origin of the lamina propria dendritic cell network. Immunity *31*, 513-525.

Castedo, M., Perfettini, J.L., Roumier, T., Andreau, K., Medema, R., and Kroemer, G. (2004). Cell death by mitotic catastrophe: a molecular definition. Oncogene *23*, 2825-2837.

Caton, M.L., Smith-Raska, M.R., and Reizis, B. (2007). Notch-RBP-J signaling controls the homeostasis of CD8- dendritic cells in the spleen. The Journal of experimental medicine *204*, 1653-1664.

Caux, C., Vanbervliet, B., Massacrier, C., Dezutter-Dambuyant, C., de Saint-Vis, B., Jacquet, C., Yoneda, K., Imamura, S., Schmitt, D., and Banchereau, J. (1996). CD34+ hematopoietic progenitors from human cord blood differentiate along two independent dendritic cell pathways in response to GM-CSF+TNF alpha. The Journal of experimental medicine *184*, 695-706.

Chardin, P., Boquet, P., Madaule, P., Popoff, M.R., Rubin, E.J., and Gill, D.M. (1989). The mammalian G protein rhoC is ADP-ribosylated by Clostridium botulinum exoenzyme C3 and affects actin microfilaments in Vero cells. The EMBO journal *8*, 1087-1092.

Charron, F., Tsimiklis, G., Arcand, M., Robitaille, L., Liang, Q., Molkentin, J.D., Meloche, S., and Nemer, M. (2001). Tissue-specific GATA factors are transcriptional effectors of the small GTPase RhoA. Genes & development *15*, 2702-2719.

Chen, M., Huang, L., and Wang, J. (2007). Deficiency of Bim in dendritic cells contributes to overactivation of lymphocytes and autoimmunity. Blood *109*, 4360-4367.

Chen, M., Wang, Y.H., Wang, Y., Huang, L., Sandoval, H., Liu, Y.J., and Wang, J. (2006). Dendritic cell apoptosis in the maintenance of immune tolerance. Science *311*, 1160-1164.

Cisse, B., Caton, M.L., Lehner, M., Maeda, T., Scheu, S., Locksley, R., Holmberg, D., Zweier, C., den Hollander, N.S., Kant, S.G.*, et al.* (2008). Transcription factor E2-2 is an essential and specific regulator of plasmacytoid dendritic cell development. Cell *135*, 37-48.

Comerford, I., Litchfield, W., Kara, E., and McColl, S.R. (2012). PI3Kgamma drives priming and survival of autoreactive CD4(+) T cells during experimental autoimmune encephalomyelitis. PloS one *7*, e45095.

Daro, E., Pulendran, B., Brasel, K., Teepe, M., Pettit, D., Lynch, D.H., Vremec, D., Robb, L.,

Shortman, K., McKenna, H.J., *et al.* (2000). Polyethylene glycol-modified GM-CSF expands CD11b(high)CD11c(high) but notCD11b(low)CD11c(high) murine dendritic cells in vivo: a comparative analysis with Flt3 ligand. Journal of immunology *165*, 49-58.

Del Prete, A., Vermi, W., Dander, E., Otero, K., Barberis, L., Luini, W., Bernasconi, S., Sironi, M., Santoro, A., Garlanda, C., *et al.* (2004). Defective dendritic cell migration and activation of adaptive immunity in PI3Kgamma-deficient mice. The EMBO journal *23*, 3505-3515.

Diao, J., Winter, E., Cantin, C., Chen, W., Xu, L., Kelvin, D., Phillips, J., and Cattral, M.S. (2006). In situ replication of immediate dendritic cell (DC) precursors contributes to conventional DC homeostasis in lymphoid tissue. Journal of immunology *176*, 7196-7206.

Diaz-Martinez, L.A., Karamysheva, Z.N., Warrington, R., Li, B., Wei, S., Xie, X.J., Roth, M.G., and Yu, H. (2014). Genome-wide siRNA screen reveals coupling between mitotic apoptosis and adaptation. The EMBO journal *33*, 1960-1976.

Dudziak, D., Kamphorst, A.O., Heidkamp, G.F., Buchholz, V.R., Trumpfheller, C., Yamazaki, S., Cheong, C., Liu, K., Lee, H.W., Park, C.G., *et al.* (2007). Differential antigen processing by dendritic cell subsets in vivo. Science *315*, 107-111.

Fogg, D.K., Sibon, C., Miled, C., Jung, S., Aucouturier, P., Littman, D.R., Cumano, A., and Geissmann, F. (2006). A clonogenic bone marrow progenitor specific for macrophages and dendritic cells. Science *311*, 83-87.

Gatto, D., Wood, K., Caminschi, I., Murphy-Durland, D., Schofield, P., Christ, D., Karupiah, G., and Brink, R. (2013). The chemotactic receptor EBI2 regulates the homeostasis, localization and immunological function of splenic dendritic cells. Nature immunology *14*, 446-453.

Geddis, A.E., Fox, N.E., Tkachenko, E., and Kaushansky, K. (2007). Endomitotic megakaryocytes that form a bipolar spindle exhibit cleavage furrow ingression followed by furrow regression. Cell cycle *6*, 455-460.

Ginhoux, F., Liu, K., Helft, J., Bogunovic, M., Greter, M., Hashimoto, D., Price, J., Yin, N., Bromberg, J., Lira, S.A., *et al.* (2009). The origin and development of nonlymphoid tissue CD103+ DCs. The Journal of experimental medicine *206*, 3115-3130.

Greter, M., Helft, J., Chow, A., Hashimoto, D., Mortha, A., Agudo-Cantero, J., Bogunovic, M., Gautier, E.L., Miller, J., Leboeuf, M., *et al.* (2012). GM-CSF controls nonlymphoid tissue dendritic cell homeostasis but is dispensable for the differentiation of inflammatory dendritic cells. Immunity *36*, 1031-1046.

Guiducci, C., Ghirelli, C., Marloie-Provost, M.A., Matray, T., Coffman, R.L., Liu, Y.J., Barrat, F.J., and Soumelis, V. (2008). PI3K is critical for the nuclear translocation of IRF-7 and type I IFN production by human plasmacytoid predendritic cells in response to TLR activation. The Journal of experimental medicine *205*, 315-322.

Heasman, S.J., and Ridley, A.J. (2008). Mammalian Rho GTPases: new insights into their

functions from in vivo studies. Nature reviews. Molecular cell biology *9*, 690-701.

Henri, S., Vremec, D., Kamath, A., Waithman, J., Williams, S., Benoist, C., Burnham, K., Saeland, S., Handman, E., and Shortman, K. (2001). The dendritic cell populations of mouse lymph nodes. Journal of immunology *167*, 741-748.

Hill, C.S., Wynne, J., and Treisman, R. (1995). The Rho family GTPases RhoA, Rac1, and CDC42Hs regulate transcriptional activation by SRF. Cell *81*, 1159-1170.

Hippenstiel, S., Schmeck, B., N'Guessan, P.D., Seybold, J., Krull, M., Preissner, K., Eichel-Streiber, C.V., and Suttorp, N. (2002). Rho protein inactivation induced apoptosis of cultured human endothelial cells. American journal of physiology. Lung cellular and molecular physiology *283*, L830-838.

Hochrein, H., Shortman, K., Vremec, D., Scott, B., Hertzog, P., and O'Keeffe, M. (2001). Differential production of IL-12, IFN-alpha, and IFN-gamma by mouse dendritic cell subsets. Journal of immunology *166*, 5448-5455.

Hou, W.S., and Van Parijs, L. (2004). A Bcl-2-dependent molecular timer regulates the lifespan and immunogenicity of dendritic cells. Nature immunology *5*, 583-589.

Inaba, K., Inaba, M., Romani, N., Aya, H., Deguchi, M., Ikehara, S., Muramatsu, S., and Steinman, R.M. (1992). Generation of large numbers of dendritic cells from mouse bone marrow cultures supplemented with granulocyte/macrophage colony-stimulating factor. The Journal of experimental medicine *176*, 1693-1702.

Iyoda, T., Shimoyama, S., Liu, K., Omatsu, Y., Akiyama, Y., Maeda, Y., Takahara, K., Steinman, R.M., and Inaba, K. (2002). The CD8+ dendritic cell subset selectively endocytoses dying cells in culture and in vivo. The Journal of experimental medicine *195*, 1289-1302.

Jackson, B., Peyrollier, K., Pedersen, E., Basse, A., Karlsson, R., Wang, Z., Lefever, T., Ochsenbein, A.M., Schmidt, G., Aktories, K.*, et al.* (2011). RhoA is dispensable for skin development, but crucial for contraction and directed migration of keratinocytes. Molecular biology of the cell *22*, 593-605.

Jaffe, A.B., and Hall, A. (2005). Rho GTPases: biochemistry and biology. Annual review of cell and developmental biology *21*, 247-269.

Johnson, C., Marriott, S.J., and Levy, L.S. (2007). Overexpression of p101 activates PI3Kgamma signaling in T cells and contributes to cell survival. Oncogene *26*, 7049-7057.

Jung, S., Unutmaz, D., Wong, P., Sano, G., De los Santos, K., Sparwasser, T., Wu, S., Vuthoori, S., Ko, K., Zavala, F.*, et al.* (2002). In vivo depletion of CD11c+ dendritic cells abrogates priming of CD8+ T cells by exogenous cell-associated antigens. Immunity *17*, 211-220.

Kabashima, K., Banks, T.A., Ansel, K.M., Lu, T.T., Ware, C.F., and Cyster, J.G. (2005). Intrinsic lymphotoxin-beta receptor requirement for homeostasis of lymphoid tissue dendritic

cells. Immunity *22*, 439-450.

Kamath, A.T., Henri, S., Battye, F., Tough, D.F., and Shortman, K. (2002). Developmental kinetics and lifespan of dendritic cells in mouse lymphoid organs. Blood *100*, 1734-1741.

Kamath, A.T., Pooley, J., O'Keeffe, M.A., Vremec, D., Zhan, Y., Lew, A.M., D'Amico, A., Wu, L., Tough, D.F., and Shortman, K. (2000). The development, maturation, and turnover rate of mouse spleen dendritic cell populations. Journal of immunology *165*, 6762-6770.

Karsunky, H., Merad, M., Cozzio, A., Weissman, I.L., and Manz, M.G. (2003). Flt3 ligand regulates dendritic cell development from Flt3+ lymphoid and myeloid-committed progenitors to Flt3+ dendritic cells in vivo. The Journal of experimental medicine *198*, 305-313.

King, I.L., Kroenke, M.A., and Segal, B.M. (2010). GM-CSF-dependent, CD103+ dermal dendritic cells play a critical role in Th effector cell differentiation after subcutaneous immunization. The Journal of experimental medicine *207*, 953-961.

Kingston, D., Schmid, M.A., Onai, N., Obata-Onai, A., Baumjohann, D., and Manz, M.G. (2009). The concerted action of GM-CSF and Flt3-ligand on in vivo dendritic cell homeostasis. Blood *114*, 835-843.

Klebanoff, C.A., Spencer, S.P., Torabi-Parizi, P., Grainger, J.R., Roychoudhuri, R., Ji, Y., Sukumar, M., Muranski, P., Scott, C.D., Hall, J.A.*, et al.* (2013). Retinoic acid controls the homeostasis of pre-cDC-derived splenic and intestinal dendritic cells. The Journal of experimental medicine *210*, 1961-1976.

Kobayashi, M., Azuma, E., Ido, M., Hirayama, M., Jiang, Q., Iwamoto, S., Kumamoto, T., Yamamoto, H., Sakurai, M., and Komada, Y. (2001). A pivotal role of Rho GTPase in the regulation of morphology and function of dendritic cells. Journal of immunology *167*, 3585-3591.

Kohno, Y., Tanimoto, A., Cirathaworn, C., Shimajiri, S., Tawara, A., and Sasaguri, Y. (2004). GM-CSF activates RhoA, integrin and MMP expression in human monocytic cells. Pathology international *54*, 693-702.

Lewis, K.L., Caton, M.L., Bogunovic, M., Greter, M., Grajkowska, L.T., Ng, D., Klinakis, A., Charo, I.F., Jung, S., Gommerman, J.L.*, et al.* (2011). Notch2 receptor signaling controls functional differentiation of dendritic cells in the spleen and intestine. Immunity *35*, 780-791.

Lin, M.L., Zhan, Y., Proietto, A.I., Prato, S., Wu, L., Heath, W.R., Villadangos, J.A., and Lew, A.M. (2008). Selective suicide of cross-presenting CD8+ dendritic cells by cytochrome c injection shows functional heterogeneity within this subset. Proceedings of the National Academy of Sciences of the United States of America *105*, 3029-3034.

Lin, Y., Roberts, T.J., Sriram, V., Cho, S., and Brutkiewicz, R.R. (2003). Myeloid marker expression on antiviral CD8+ T cells following an acute virus infection. European journal of immunology *33*, 2736-2743.

Liu, K., and Nussenzweig, M.C. (2010). Origin and development of dendritic cells. Immunological reviews *234*, 45-54.

Liu, K., Victora, G.D., Schwickert, T.A., Guermonprez, P., Meredith, M.M., Yao, K., Chu, F.F., Randolph, G.J., Rudensky, A.Y., and Nussenzweig, M. (2009). In vivo analysis of dendritic cell development and homeostasis. Science *324*, 392-397.

Liu, K., Waskow, C., Liu, X., Yao, K., Hoh, J., and Nussenzweig, M. (2007). Origin of dendritic cells in peripheral lymphoid organs of mice. Nature immunology *8*, 578-583.

Liu, Y.J. (2005). IPC: professional type 1 interferon-producing cells and plasmacytoid dendritic cell precursors. Annual review of immunology *23*, 275-306.

Lordier, L., Jalil, A., Aurade, F., Larbret, F., Larghero, J., Debili, N., Vainchenker, W., and Chang, Y. (2008). Megakaryocyte endomitosis is a failure of late cytokinesis related to defects in the contractile ring and Rho/Rock signaling. Blood *112*, 3164-3174.

Maldonado-Lopez, R., De Smedt, T., Michel, P., Godfroid, J., Pajak, B., Heirman, C., Thielemans, K., Leo, O., Urbain, J., and Moser, M. (1999). CD8alpha+ and CD8alpha- subclasses of dendritic cells direct the development of distinct T helper cells in vivo. The Journal of experimental medicine *189*, 587-592.

Mali, R.S., Ramdas, B., Ma, P., Shi, J., Munugalavadla, V., Sims, E., Wei, L., Vemula, S., Nabinger, S.C., Goodwin, C.B.*, et al.* (2011). Rho kinase regulates the survival and transformation of cells bearing oncogenic forms of KIT, FLT3, and BCR-ABL. Cancer cell *20*, 357-369.

Maraskovsky, E., Brasel, K., Teepe, M., Roux, E.R., Lyman, S.D., Shortman, K., and McKenna, H.J. (1996). Dramatic increase in the numbers of functionally mature dendritic cells in Flt3 ligand-treated mice: multiple dendritic cell subpopulations identified. The Journal of experimental medicine *184*, 1953-1962.

McKenna, H.J., Stocking, K.L., Miller, R.E., Brasel, K., De Smedt, T., Maraskovsky, E., Maliszewski, C.R., Lynch, D.H., Smith, J., Pulendran, B.*, et al.* (2000). Mice lacking flt3 ligand have deficient hematopoiesis affecting hematopoietic progenitor cells, dendritic cells, and natural killer cells. Blood *95*, 3489-3497.

Melendez, J., Stengel, K., Zhou, X., Chauhan, B.K., Debidda, M., Andreassen, P., Lang, R.A., and Zheng, Y. (2011). RhoA GTPase is dispensable for actomyosin regulation but is essential for mitosis in primary mouse embryonic fibroblasts. The Journal of biological chemistry *286*, 15132-15137.

Merad, M., Sathe, P., Helft, J., Miller, J., and Mortha, A. (2013). The dendritic cell lineage: ontogeny and function of dendritic cells and their subsets in the steady state and the inflamed setting. Annual review of immunology *31*, 563-604.

Miller, N.L., Lawson, C., Chen, X.L., Lim, S.T., and Schlaepfer, D.D. (2012). Rgnef (p190RhoGEF) knockout inhibits RhoA activity, focal adhesion establishment, and cell

motility downstream of integrins. PloS one *7*, e37830.

Mohr, C., Koch, G., Just, I., and Aktories, K. (1992). ADP-ribosylation by Clostridium botulinum C3 exoenzyme increases steady-state GTPase activities of recombinant rhoA and rhoB proteins. FEBS letters *297*, 95-99.

Muessel, M.J., Scott, K.S., Friedl, P., Bradding, P., and Wardlaw, A.J. (2008). CCL11 and GM-CSF differentially use the Rho GTPase pathway to regulate motility of human eosinophils in a three-dimensional microenvironment. Journal of immunology *180*, 8354-8360.

Naik, S.H., Metcalf, D., van Nieuwenhuijze, A., Wicks, I., Wu, L., O'Keeffe, M., and Shortman, K. (2006). Intrasplenic steady-state dendritic cell precursors that are distinct from monocytes. Nature immunology *7*, 663-671.

Naik, S.H., Sathe, P., Park, H.Y., Metcalf, D., Proietto, A.I., Dakic, A., Carotta, S., O'Keeffe, M., Bahlo, M., Papenfuss, A*., et al.* (2007). Development of plasmacytoid and conventional dendritic cell subtypes from single precursor cells derived in vitro and in vivo. Nature immunology *8*, 1217-1226.

Nopora, A., and Brocker, T. (2002). Bcl-2 controls dendritic cell longevity in vivo. Journal of immunology *169*, 3006-3014.

O'Keeffe, M., Hochrein, H., Vremec, D., Caminschi, I., Miller, J.L., Anders, E.M., Wu, L., Lahoud, M.H., Henri, S., Scott, B*., et al.* (2002). Mouse plasmacytoid cells: long-lived cells, heterogeneous in surface phenotype and function, that differentiate into CD8(+) dendritic cells only after microbial stimulus. The Journal of experimental medicine *196*, 1307-1319.

Ocana-Morgner, C., Reichardt, P., Chopin, M., Braungart, S., Wahren, C., Gunzer, M., and Jessberger, R. (2011). Sphingosine 1-phosphate-induced motility and endocytosis of dendritic cells is regulated by SWAP-70 through RhoA. Journal of immunology *186*, 5345-5355.

Ocana-Morgner, C., Wahren, C., and Jessberger, R. (2009). SWAP-70 regulates RhoA/RhoB-dependent MHCII surface localization in dendritic cells. Blood *113*, 1474-1482.

Ohnmacht, C., Pullner, A., King, S.B., Drexler, I., Meier, S., Brocker, T., and Voehringer, D. (2009). Constitutive ablation of dendritic cells breaks self-tolerance of CD4 T cells and results in spontaneous fatal autoimmunity. The Journal of experimental medicine *206*, 549-559.

Olson, M.F., Ashworth, A., and Hall, A. (1995). An essential role for Rho, Rac, and Cdc42 GTPases in cell cycle progression through G1. Science *269*, 1270-1272.

Onai, N., Kurabayashi, K., Hosoi-Amaike, M., Toyama-Sorimachi, N., Matsushima, K., Inaba, K., and Ohteki, T. (2013). A clonogenic progenitor with prominent plasmacytoid dendritic cell developmental potential. Immunity *38*, 943-957.

Onai, N., Obata-Onai, A., Schmid, M.A., Ohteki, T., Jarrossay, D., and Manz, M.G. (2007). Identification of clonogenic common Flt3+M-CSFR+ plasmacytoid and conventional dendritic cell progenitors in mouse bone marrow. Nature immunology *8*, 1207-1216.

Park, D., Lapteva, N., Seethammagari, M., Slawin, K.M., and Spencer, D.M. (2006). An essential role for Akt1 in dendritic cell function and tumor immunotherapy. Nature biotechnology *24*, 1581-1590.

Pille, J.Y., Denoyelle, C., Varet, J., Bertrand, J.R., Soria, J., Opolon, P., Lu, H., Pritchard, L.L., Vannier, J.P., Malvy, C.*, et al.* (2005). Anti-RhoA and anti-RhoC siRNAs inhibit the proliferation and invasiveness of MDA-MB-231 breast cancer cells in vitro and in vivo. Molecular therapy : the journal of the American Society of Gene Therapy *11*, 267-274.

Pulendran, B., Smith, J.L., Caspary, G., Brasel, K., Pettit, D., Maraskovsky, E., and Maliszewski, C.R. (1999). Distinct dendritic cell subsets differentially regulate the class of immune response in vivo. Proceedings of the National Academy of Sciences of the United States of America *96*, 1036-1041.

Rappsilber, J., Mann, M., and Ishihama, Y. (2007). Protocol for micro-purification, enrichment, pre-fractionation and storage of peptides for proteomics using StageTips. Nature protocols *2*, 1896-1906.

Reis e Sousa, C. (2006). Dendritic cells in a mature age. Nature reviews. Immunology *6*, 476-483.

Reizis, B., Colonna, M., Trinchieri, G., Barrat, F., and Gilliet, M. (2011). Plasmacytoid dendritic cells: one-trick ponies or workhorses of the immune system? Nature reviews. Immunology *11*, 558-565.

Reuveny, M., Heller, H., and Bengal, E. (2004). RhoA controls myoblast survival by inducing the phosphatidylinositol 3-kinase-Akt signaling pathway. FEBS letters *569*, 129-134.

Rodrigues, D.H., Vilela, M.C., Barcelos, L.S., Pinho, V., Teixeira, M.M., and Teixeira, A.L. (2010). Absence of PI3Kgamma leads to increased leukocyte apoptosis and diminished severity of experimental autoimmune encephalomyelitis. Journal of neuroimmunology *222*, 90-94.

Ruedl, C., Koebel, P., Bachmann, M., Hess, M., and Karjalainen, K. (2000). Anatomical origin of dendritic cells determines their life span in peripheral lymph nodes. Journal of immunology *165*, 4910-4916.

Sahai, E., and Marshall, C.J. (2002). RHO-GTPases and cancer. Nature reviews. Cancer *2*, 133-142.

Sallusto, F., and Lanzavecchia, A. (1994). Efficient presentation of soluble antigen by cultured human dendritic cells is maintained by granulocyte/macrophage colony-stimulating factor plus interleukin 4 and downregulated by tumor necrosis factor alpha. The Journal of experimental medicine *179*, 1109-1118.

Satpathy, A.T., Wu, X., Albring, J.C., and Murphy, K.M. (2012). Re(de)fining the dendritic cell lineage. Nature immunology *13*, 1145-1154.

Schulz, O., and Reis e Sousa, C. (2002). Cross-presentation of cell-associated antigens by CD8alpha+ dendritic cells is attributable to their ability to internalize dead cells. Immunology *107*, 183-189.

She, Q.B., Solit, D.B., Ye, Q., O'Reilly, K.E., Lobo, J., and Rosen, N. (2005). The BAD protein integrates survival signaling by EGFR/MAPK and PI3K/Akt kinase pathways in PTEN-deficient tumor cells. Cancer cell *8*, 287-297.

Shortman, K., and Heath, W.R. (2010). The CD8+ dendritic cell subset. Immunological reviews *234*, 18-31.

Shortman, K., and Liu, Y.J. (2002). Mouse and human dendritic cell subtypes. Nature reviews. Immunology *2*, 151-161.

Shortman, K., and Naik, S.H. (2007). Steady-state and inflammatory dendritic-cell development. Nature reviews. Immunology *7*, 19-30.

Shurin, G.V., Tourkova, I.L., Chatta, G.S., Schmidt, G., Wei, S., Djeu, J.Y., and Shurin, M.R. (2005). Small rho GTPases regulate antigen presentation in dendritic cells. Journal of immunology *174*, 3394-3400.

Shuster, C.B., and Burgess, D.R. (1999). Parameters that specify the timing of cytokinesis. The Journal of cell biology *146*, 981-992.

Steinman, R.M., and Cohn, Z.A. (1973). Identification of a novel cell type in peripheral lymphoid organs of mice. I. Morphology, quantitation, tissue distribution. The Journal of experimental medicine *137*, 1142-1162.

Steinman, R.M., and Cohn, Z.A. (1974). Identification of a novel cell type in peripheral lymphoid organs of mice. II. Functional properties in vitro. The Journal of experimental medicine *139*, 380-397.

Stranges, P.B., Watson, J., Cooper, C.J., Choisy-Rossi, C.M., Stonebraker, A.C., Beighton, R.A., Hartig, H., Sundberg, J.P., Servick, S., Kaufmann, G.*, et al.* (2007). Elimination of antigen-presenting cells and autoreactive T cells by Fas contributes to prevention of autoimmunity. Immunity *26*, 629-641.

Tybulewicz, V.L., and Henderson, R.B. (2009). Rho family GTPases and their regulators in lymphocytes. Nature reviews. Immunology *9*, 630-644.

Vandenabeele, P., Galluzzi, L., Vanden Berghe, T., and Kroemer, G. (2010). Molecular mechanisms of necroptosis: an ordered cellular explosion. Nature reviews. Molecular cell biology *11*, 700-714.

Vizcaino, J.A., Deutsch, E.W., Wang, R., Csordas, A., Reisinger, F., Rios, D., Dianes, J.A., Sun, Z., Farrah, T., Bandeira, N.*, et al.* (2014). ProteomeXchange provides globally coordinated proteomics data submission and dissemination. Nature biotechnology *32*, 223-226.

Vremec, D., Lieschke, G.J., Dunn, A.R., Robb, L., Metcalf, D., and Shortman, K. (1997). The influence of granulocyte/macrophage colony-stimulating factor on dendritic cell levels in mouse lymphoid organs. European journal of immunology *27*, 40-44.

Vremec, D., Pooley, J., Hochrein, H., Wu, L., and Shortman, K. (2000). CD4 and CD8 expression by dendritic cell subtypes in mouse thymus and spleen. Journal of immunology *164*, 2978-2986.

Wang, L., and Zheng, Y. (2007). Cell type-specific functions of Rho GTPases revealed by gene targeting in mice. Trends in cell biology *17*, 58-64.

Wang, Y.G., Kim, K.D., Wang, J., Yu, P., and Fu, Y.X. (2005). Stimulating lymphotoxin beta receptor on the dendritic cells is critical for their homeostasis and expansion. Journal of immunology *175*, 6997-7002.

Wang, Z., Kumamoto, Y., Wang, P., Gan, X., Lehmann, D., Smrcka, A.V., Cohn, L., Iwasaki, A., Li, L., and Wu, D. (2009). Regulation of immature dendritic cell migration by RhoA guanine nucleotide exchange factor Arhgef5. The Journal of biological chemistry *284*, 28599-28606.

Waskow, C., Liu, K., Darrasse-Jeze, G., Guermonprez, P., Ginhoux, F., Merad, M., Shengelia, T., Yao, K., and Nussenzweig, M. (2008). The receptor tyrosine kinase Flt3 is required for dendritic cell development in peripheral lymphoid tissues. Nature immunology *9*, 676-683.

Wisniewski, J.R., Zougman, A., and Mann, M. (2009a). Combination of FASP and StageTip-based fractionation allows in-depth analysis of the hippocampal membrane proteome. Journal of proteome research *8*, 5674-5678.

Wisniewski, J.R., Zougman, A., Nagaraj, N., and Mann, M. (2009b). Universal sample preparation method for proteome analysis. Nature methods *6*, 359-362.

Worthylake, R.A., and Burridge, K. (2003). RhoA and ROCK promote migration by limiting membrane protrusions. The Journal of biological chemistry *278*, 13578-13584.

Yi, T., and Cyster, J.G. (2013). EBI2-mediated bridging channel positioning supports splenic dendritic cell homeostasis and particulate antigen capture. eLife *2*, e00757.

Yoneyama, H., Matsuno, K., Zhang, Y., Nishiwaki, T., Kitabatake, M., Ueha, S., Narumi, S., Morikawa, S., Ezaki, T., Lu, B.*, et al.* (2004). Evidence for recruitment of plasmacytoid dendritic cell precursors to inflamed lymph nodes through high endothelial venules. International immunology *16*, 915-928.

Zhang, J., Raper, A., Sugita, N., Hingorani, R., Salio, M., Palmowski, M.J., Cerundolo, V., and Crocker, P.R. (2006). Characterization of Siglec-H as a novel endocytic receptor expressed on murine plasmacytoid dendritic cell precursors. Blood *107*, 3600-3608.

Zhang, S., Zhou, X., Lang, R.A., and Guo, F. (2012). RhoA of the Rho family small GTPases is essential for B lymphocyte development. PloS one *7*, e33773.

Zhou, X., Florian, M.C., Arumugam, P., Chen, X., Cancelas, J.A., Lang, R., Malik, P., Geiger, H., and Zheng, Y. (2013). RhoA GTPase controls cytokinesis and programmed necrosis of hematopoietic progenitors. The Journal of experimental medicine *210*, 2371-2385.

Zhou, X., and Zheng, Y. (2013). Cell type-specific signaling function of RhoA GTPase: lessons from mouse gene targeting. The Journal of biological chemistry *288*, 36179-36188.

Zhu, S., Korzh, V., Gong, Z., and Low, B.C. (2008). RhoA prevents apoptosis during zebrafish embryogenesis through activation of Mek/Erk pathway. Oncogene *27*, 1580-1589.

10. CURRICULUM VITAE

Personal information:

Name   Shuai Li

Date of birth   23 November 1983

Place of birth   Linfen, Shanxi, China

Nationality   China

E-mail   lishuai305@gmail.com

Education:

Since 09/2011	**PhD in Immunology** Prof. Dr. Thomas Brocker, Institute for Immunology, LMU, Munich, Germany Thesis title: Control of homeostasis of dendritic cell by the GTPase RhoA
09/2008 - 07/2011	**Master in Preventive Veterinary Medicine** Prof. Aizhen Guo, National Key Laboratory of Agricultural Microbiology, Huazhong Agricultural University, Wuhan, China Thesis title: *Mycobacterium bovis* and BCG induce different patterns of cytokine and chemokine production in dendritic cells and differentiation patterns in CD4$^+$ T cells
09/2004 - 07/2008	**Bachelor in Biology** Shanxi Agricultural University, Shanxi, China

Conferences:

04/2013	SFB914 retreat, *Obergurgl, Austria*
03/2014	International Conference on Leukocyte Trafficking, *Munich, Germany*
09/2014	DC Conference 2014, *Tours, France*
01/2015	Midwinter Conference: Advances in Immunology, *Seefeld, Austria*

11. ACKNOWLEDGMENTS